AD_____

Award Number: W81XWH -12-2-0083

TITLE: Persistence of Antibiotic Resistance Plasmids in Biofilms

PRINCIPAL INVESTIGATOR: Dr. Eva Top

CONTRACTING ORGANIZATION: University of Idaho, Moscow, ID 83844

REPORT DATE: October 2014

TYPE OF REPORT: Annual Report

PREPARED FOR: U.S. Army Medical Research and Materiel Command
Fort Detrick, Maryland 21702-5012

DISTRIBUTION STATEMENT: Approved for Public Release;
Distribution Unlimited

REPORT DOCUMENTATION PAGE

Form Approved
OMB No. 0704-0188

1. REPORT DATE	**2. REPORT TYPE**	**3. DATES COVERED**
October 20142014	Annual	30 Sep 2013 – 29 Sep 2014

4. TITLE AND SUBTITLE

Persistence of Antibiotic Resistance Plasmids in Biofilms

5a. CONTRACT NUMBER

5b. GRANT NUMBER
W81XWH -12-2-0083

5c. PROGRAM ELEMENT NUMBER

6. AUTHOR(S)
Dr. Eva M. Top, Dr. Ben Ridenhour

E-Mail: evatop@uidaho.edu

5d. PROJECT NUMBER

5e. TASK NUMBER

5f. WORK UNIT NUMBER

7. PERFORMING ORGANIZATION NAME(S) AND ADDRESS(ES)

Department of Biological Sciences
Institute of Bioinformatics and Evolutionary Studies (IBEST)
University of Idaho
875 Perimeter Drive MS 3051
Moscow ID 83844-3051
Phone: 1-208-885-5015

8. PERFORMING ORGANIZATION REPORT NUMBER

9. SPONSORING / MONITORING AGENCY NAME(S) AND ADDRESS(ES)
U.S. Army Medical Research and Material Command
Fort Detrick, Maryland 21702-5012

10. SPONSOR/MONITOR'S ACRONYM(S)
USAMRMC

11. SPONSOR/MONITOR'S REPORT NUMBER(S)

12. DISTRIBUTION / AVAILABILITY STATEMENT
Approved for Public Release; Distribution Unlimited

13. SUPPLEMENTARY NOTES

14. ABSTRACT

Plasmids play an important role in the spread of genes that confer resistance to antibiotics among bacterial pathogens. Given the worrisome rise of bacterial multi-drug resistance worldwide, the goal of our current research project is to characterize the evolutionary mechanisms by which multi-drug resistance (MDR) plasmids improve their persistence in biofilms formed by important wound pathogens. The central hypothesis of this study is that the evolutionary pathways through which stable plasmid maintenance improves are different and more varied in biofilms than in well-mixed liquid cultures due to the uniquely spatially structured environment of biofilms. To address this hypotheses the following aims are being addressed: (i) Compare the persistence of MDR plasmids in populations of clinically relevant bacteria grown in biofilms and well-mixed liquid cultures; (ii) Compare the evolution of plasmid persistence in bacteria grown in biofilms and well-mixed liquids; (iii) Characterize evolutionary changes that occur during stabilization of plasmid-host pairs under both conditions.

We have accomplished several aspects of all tasks outlined in the SOW. Our preliminary results indicate that the structured biofilm environment, which typically characterizes the type of bacterial growth in wounds, facilitates the persistence of MDR plasmids in *Acinetobacter baumannii,* a problematic wound pathogen. Moreover, we have shown that plasmids coevolved with their host under antibiotic selection for 28 days have improved their persistence in part by undergoing large structural changes. While still partially uncharacterized, these genetic modifications likely decrease plasmid cost to the host while retaining favorable plasmid-encoded traits (i.e. antibiotic resistance). Through whole genome resequencing we have further characterized these structural changes and other possible mutations in populations evolved in biofilms as well as in liquids. This project already greatly contributes to our understanding of the pathways through which plasmid persistence can improve in *Acinetobacter baumannii* and other wound pathogens when grown in biofilm environments.

This project has the potential of supporting future research on therapeutic agents targeting maintenance and spread of MDR plasmids. Such therapies will ultimately be useful in the care of patients with combat-related wound infections.

15. SUBJECT TERMS

Antibiotic resistance, plasmid, biofilm, coevolution, bacteria, wound infections.

16. SECURITY CLASSIFICATION OF:			**17. LIMITATION OF ABSTRACT**	**18. NUMBER OF PAGES**	**19a. NAME OF RESPONSIBLE PERSON** USAMRMC
a. REPORT U	**b. ABSTRACT** U	**c. THIS PAGE** U	UU	35	**19b. TELEPHONE NUMBER** *(include area code)*

Table of Contents

1. INTRODUCTION:

Infections of wounds sustained during combat may compromise an individual's survival by leading to septicemia. This process is complicated if the infection is caused by multi-drug resistant (MDR) Gram-negative bacteria that form biofilms in the wounds, such as *Pseudomonas aeruginosa*, *Acinetobacter baumannii*, *Klebsiella pneumoniae*, *Enterobacter* sp., and *Escherichia coli* (Eardley et al., 2011; Gaynes & Edwards, 2005; Murray, 2008). Plasmids play an important role in the spread of genes that confer antibiotic resistance among bacterial pathogens. In spite of the worrisome rise of bacterial multi-drug resistance worldwide, it is still not known how resistance plasmids are successfully maintained in the absence of antibiotic selection in bacterial populations that grow as biofilms. Therefore, understanding the genetic mechanisms involved in the evolution of plasmid stability in biofilms is critical in our search for targets for alternative therapeutic approaches. The goal of this research project is to characterize the evolutionary mechanisms by which multi-drug resistance (MDR) plasmids can improve their persistence in biofilms formed by various Gram-negative bacteria. The central hypothesis of this study is that the evolutionary pathways through which stable plasmid maintenance improves are different and more varied in biofilms than in well-mixed liquid cultures due to the uniquely spatially structured environment of biofilms. We propose the following research tasks:

Task 1: Compare the persistence of naturally occurring MDR plasmids in populations of Gram-negative bacteria grown in biofilms and well-mixed liquid cultures.

Task 2: Characterize the evolution of plasmid stability in bacterial hosts grown in biofilms and well-mixed liquid cultures.

Task 3: Characterize evolutionary changes that occur during stabilization of plasmid-host pairs in biofilms and well-mixed liquid cultures.

This proposed work has the potential of supporting future research on drug therapies that are based on restricting the dissemination and stable replication of MDR plasmids (Baquero et al., 2011). Such therapies will ultimately be useful in the care of patients with combat-related wound infections, which would have otherwise have been difficult to treat.

2. KEYWORDS:

Antibiotic resistance, plasmid, biofilm, coevolution, bacteria, wound infections

3. OVERALL PROJECT SUMMARY:

The successful persistence and therefore spread of a multi-drug resistance (MDR) plasmid in a given bacterial population or community is typically due to its ability to efficiently replicate, segregate among daughter cells, confer a low fitness cost, and horizontally transfer by conjugation. We hypothesize that an additional major factor affecting plasmid persistence is the spatial structure of the environment. In well-mixed liquid batch cultures, typically used in the laboratory to study microbial evolution and plasmid stability, newly arising mutants with beneficial mutations can rapidly increase their proportions in the population. This is due to their ability to easily outcompete their ancestral host and other less fit mutants in this will-mixed system. Such take-over of a mutant is called a 'sweep'. In contrast, the same mutants may not readily sweep through the bacterial population in a spatially structured environment such as a bacterial biofilm, because competition is local and not global. This provides opportunity for other, potentially fitter, mutants to arise and accumulate in the biofilm. As described in the SOW, we have proposed to conduct three research tasks that will allow us to better understand the mechanisms underlying evolution of plasmid persistence in biofilms as compared to liquid mixed cultures. A fourth task related to dissemination of results is also part of the SOW. The three research tasks are as follows:

Task1: Compare the persistence of naturally occurring multi-drug resistance (MDR) plasmids in populations of Gram-negative bacteria grown in biofilms and well-mixed liquid cultures.

Task2: Characterize the evolution of plasmid stability in bacterial hosts grown in biofilms and well-mixed liquid cultures.

Task 3. Characterize evolutionary changes that occur during stabilization of plasmid-host pairs in biofilms and well-mixed cultures.

The overarching goal of this project is to identify the pathways by which MDR plasmids evolve improved stability in a novel host. Addressing this question requires that we understand whether the mechanisms involved are 1) host-dependent, 2) plasmid-dependent), or 3) both. To this end, we co-evolved *Acinetobacter baumannii* with a chosen model MDR plasmid pB10 (Schlueter *et al.,* 2004) under antibiotic selection and are analyzing the phenotype and genotypic changes that may explain improvement of plasmid persistence.

Progress and results to-date are given in the following subsections for each task.

A. Task 1

We have previously completed assays to determine the persistence of wild-type plasmid pB10 in the ancestral *A. baumannii* strain used to start all evolution experiments (*Acinetobacter baumannii* ATCC 17978). These results, based on antibiotic resistance phenotypes, indicate that, prior to evolution in this host, the plasmid is rather unstable and persists in less than 2% of cells after 5 days growth in well-mixed liquid cultures without antibiotics, and around 0.1% after 10 days. We are now using high-throughput quantitative real-time PCR (qPCR) reactions to assay stability instead of the labor-intensive plate count

method for the remainder of the persistence assays in this project. We have confirmed these findings using this method.

Description of stability assay involving qPCR

As an alternative to traditional plating techniques, we developed a real-time quantitative PCR (qPCR) protocol as a sensitive and high-throughput method to quantify the relative abundance of plasmids in bacterial populations. This method is based on our recent study, which compared multiple methods to measure plasmid persistence (Loftie-Eaton *et al.*, 2014). Our method combines automatic DNA extractions with the QIAsymphony robot (QIAgen Inc.) and qPCR assays using primers for the 16S rRNA gene (located on the chromosome) and *trfA* (on the pB10 plasmid) genes. It is necessary to use a chromosomal primer (and not just plasmid based *trfA* primer) to control for the concentration of *A. baumannii* cells that was used in the DNA extraction step; the ratio of *trfA* to 16S rRNA gene copies determines the fraction of plasmid-bearing cells in the culture. Our approach allows us to isolate DNA from as little as 5 µl of bacterial cultures, and the robot provides highly reproducible and reliable means of obtaining high quality DNA later used as templates for qPCR. As an added bonus, assessment of plasmid to chromosome ratio with our high-throughput method does not rely on labor-intensive plating or colony replication methods and overnight incubations, and is less prone to human errors associated with these traditional methods.

We tested robotic DNA extractions and qPCR procedures with our ancestral *A. baumannii* strain carrying the (ancestral) pB10 plasmid, which was grown overnight in broth supplemented with antibiotics. This ancestral host-plasmid pair is hereafter referred to as DOD67. DNA extraction was optimized based on OD600 reads; qPCR was optimized for template concentrations and primer combinations. After optimization, baseline plasmid-to-chromosome ratios were established with qPCR using DNA extracted from DOD67; doing so has allowed us to use DOD67 to create standard curves (positive controls) for subsequent qPCR reactions. On day 0 of the stability assay after growth in medium with antibiotics, prior experience showed that the fraction of plasmid-bearing cells was typically 1. Because of this we decided to express the ratio of *trfA* to 16S rRNA from our qPCR assay as values relative to estimated ratio on day 0.,We compared qPCR results to our previous culture-based plasmid stability assays. We found that our DNA robot-qPCR method estimation of the fraction of plasmid bearing cells relative to that on day 0 correlates well with the data obtained from traditional culture-based methods (Fig. 1).

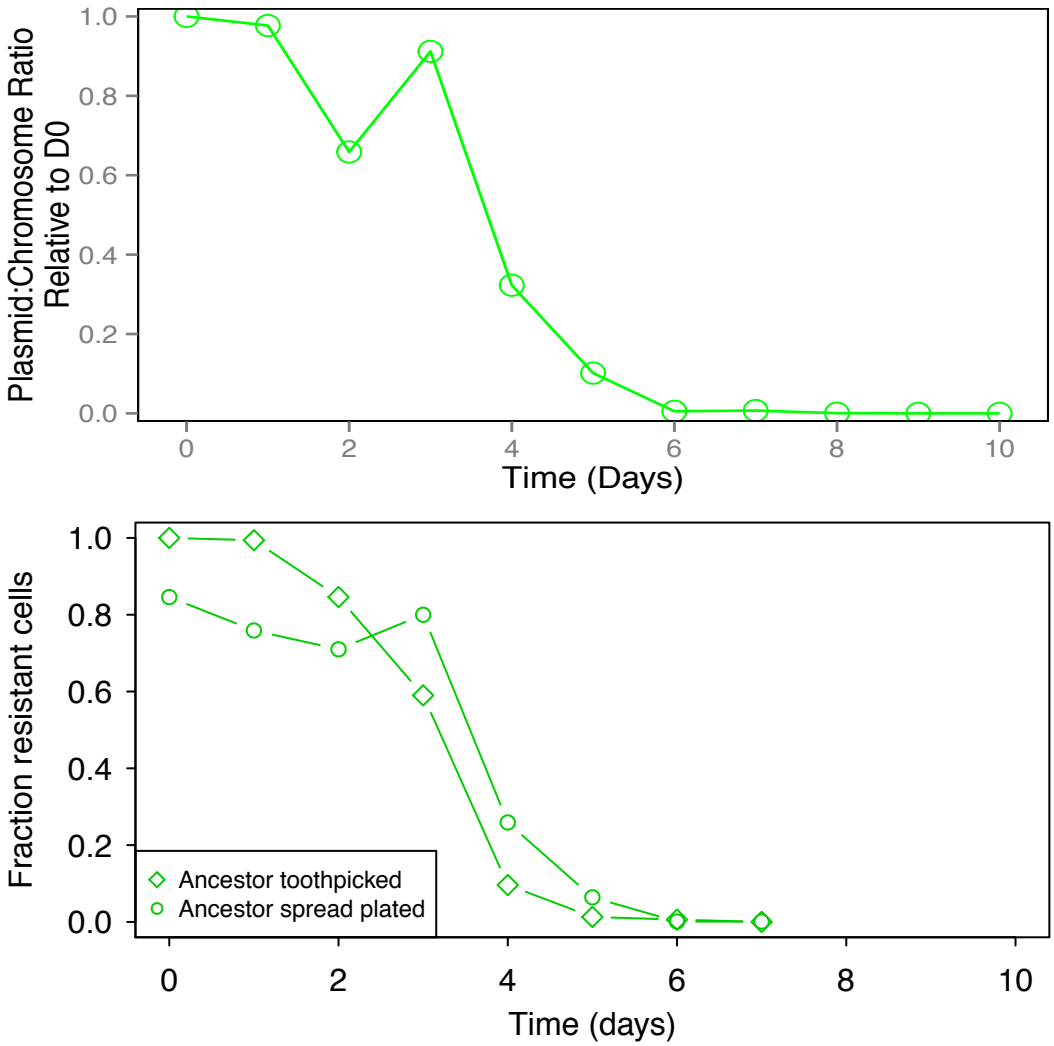

Figure 1. Comparison of qPCR assay results (top) to resistant colony based plating assays (bottom; either using colony replication ("toothpicked") or spread-plating on media with and without antibiotics) in the experimental ancestor (DOD67). Results are very similar: the time until 50% of the population has lost its plasmid is less than 4 days, and by day 5 only 10% or less of the populations still contained the plasmid.

B. Task 2

As explained in previous reports, because of the problems we encountered with loss of fluorescence encoded by *gfp*, and the interesting deletions and chromosomal integrations that occurred with the *gfp*-marked plasmid pB10::*gfp*, we are repeating a portion of the work but with the natural, unmarked plasmid pB10. Our updated workflow is now shown in Figure 2. The biggest differences are the use of qPCR to assess plasmid stability (because the plasmid now lacks *gfp* to aid in quantitation) and shortening the length of the experiment from 50 days to 28 days (because previous work indicated 28 days was long enough to observe significant host-plasmid evolution). We also now chose to apply antibiotic selection during the first four days of biofilm establishment to reduce the chance of starting out the biofilms with a mixture of plasmid-free and plasmid-bearing cells, and use these so-called 'T0' cultures as inocula for the liquid culture experiments to ensure starting populations that were as similar as possible (see arrows in Figure 2, bottom).

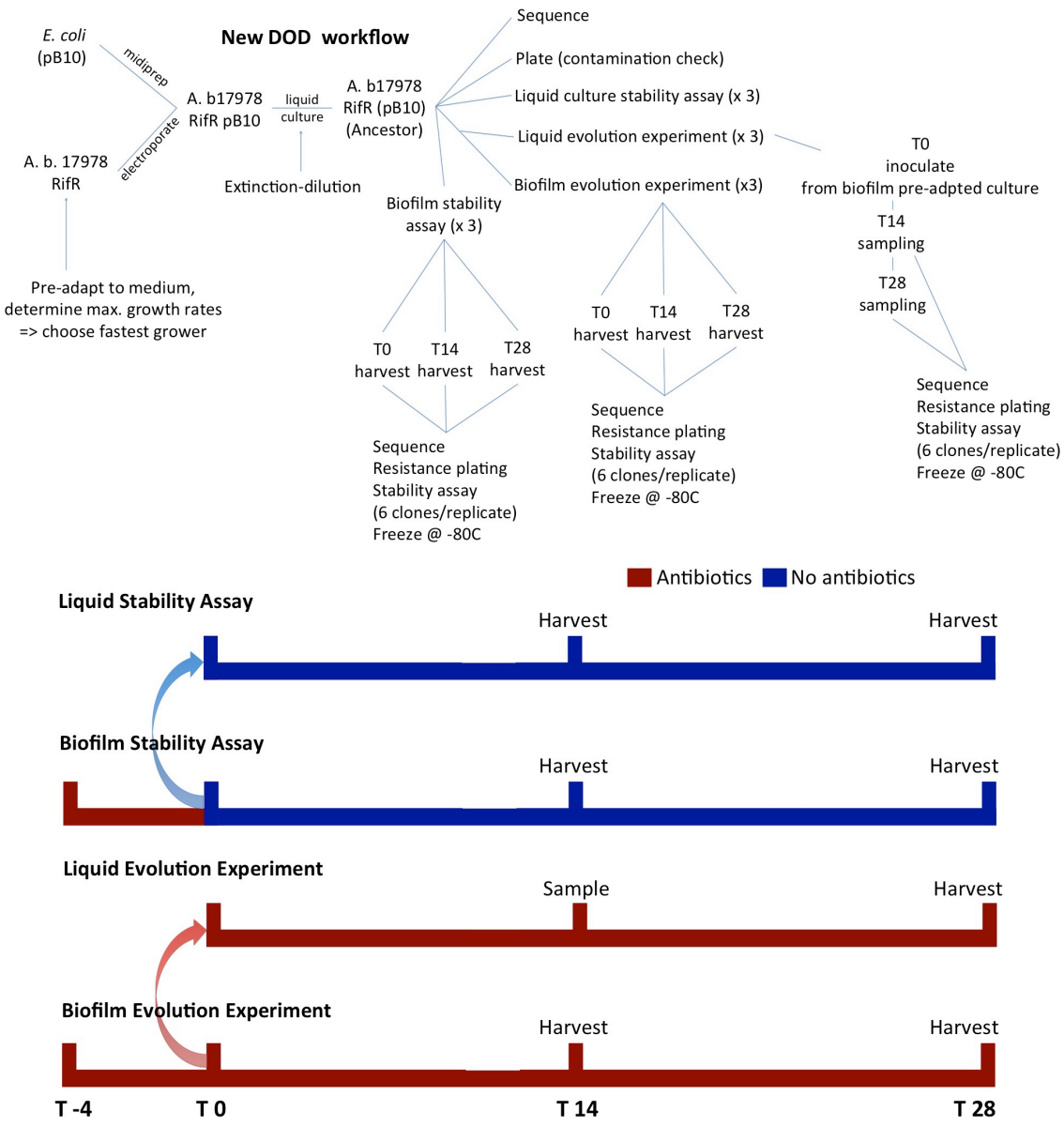

Figure 2. Updated workflows and experimental design to the project based on experience gained in the first year and a half of experimentation. Notable differences include the use of a pB10 plasmid lacking a *gfp* gene, shortening experimental time from 50 to 28 days, and the use of qPCR assays in assessing stability. The arrows indicate that the 4-day old biofilms at 'T0' are used as inocula for liquid culture experiments to ensure starting populations that are as similar as possible.

Our tandem DNA robot-qPCR assay was successfully applied to determine the stability of plasmid pB10 in our *A. baumannii* host at the beginning and end of the evolution experiments under antibiotic selection (Figure 2, red lines, T0 and T28). Briefly, at days T0, T14, and T28, the biofilms and liquid cultures were harvested, diluted and plated, and six randomly chosen colonies per replicate biofilm and liquid culture were archived at -80 C. The stability of pB10 in these clones was subsequently determined by using the frozen stocks as inocula for serial passage in liquid media without antibiotics (i.e. plasmid stability assays). Aliquots of bacterial cultures were archived daily throughout the course of the plasmid persistence assay (day 0 to day 9). A small portion (5 µl) was used for DNA isolation with QIAsymphony robot. Using 10µl qPCR reactions, plasmid-to-chromosome ratios have now been estimated for several of experimental time points. Specifically, stability assays have been done so far for six clones from one replicate each of the T0 and T28 time points for the biofilm and liquid evolution experiments, with two more replicates (=6 x 2 x 2 clones) to be analyzed in the coming weeks. Because it would be too expensive run the qPCR assay for every day of the assay (days 0-9), we identified days 0, 5 and 8 as sufficient for determining a resistance profile; samples have been retained in the freezer for the other days of assay (e.g. day 1) in case further analysis is needed. Most clones evolved in one of the replicate biofilms harvested on T28 showed dramatic improvement in stability (Figure 3). The results also suggest a larger diversity in phenotypes, with two clones showing extremely, stable plasmids. Interestingly gel electrophoresis showed that in these clones (5 and 6) pB10 underwent large deletions. Due to some technical problems, the data for evolution in liquids at T28 are currently being analyzed but preliminary data are shown in Figure 4. These data indicate that all clones evolved increased plasmid stability in liquid culture; furthermore, there seems to be a relatively consistent stability profile across all assays of the T28-liquid culture (Fig. 4).

In parallel, to obtain DNA for complete resequencing of the evolved genomes using Illumina MiSeq shotgun sequencing (part of Task 3), DNA has been extracted from 100µl of culture for six clones from one replicate of T0, T28-biofilm, and T28-liquid, using DNA purification kits (Sigma Inc.).

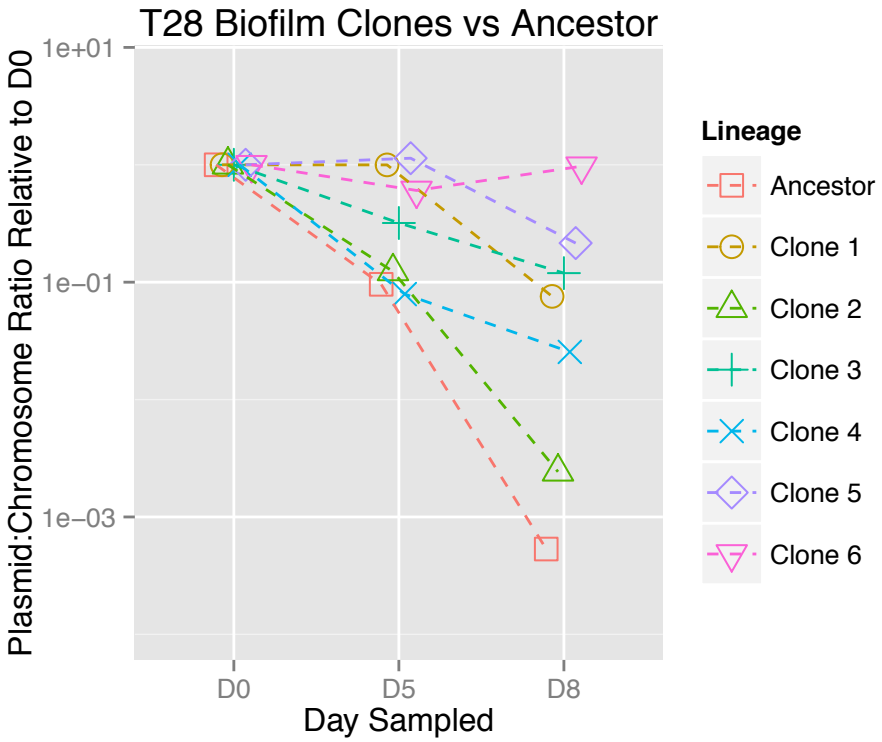

Figure 3. Plasmid stability in plasmid-host pairs from one T28 biofilm replicate evolved in the presence of antibiotics. All pairs showed improvement over the ancestral state (DOD67; red box). Clones 3, 5, and 6 showed the most improvement in stability; interestingly based on gel electrophoresis of extracted plasmid DNA and whole genome sequence analysis, pB10 derivatives in clones 5 and 6 showed large deletions (see Task 3).

Methods for analyzing the collected qPCR data have been developed in order to provide consistent results. All analyses are being conducted on raw data from the qPCR machine utilizing R. R scripts for the analyses of these raw data can be found in the Appendix. In general, a data analysis pipeline has been created so that qPCR data can be quickly and reproducibly analyzed to give estimates of plasmid stability. qPCR data are currently being collected in for other portions of the experiment. For example, T0 has partially been analyzed (2 of 6 clones) as well as T28 from the liquid evolution experiment (1 of 6 clones).

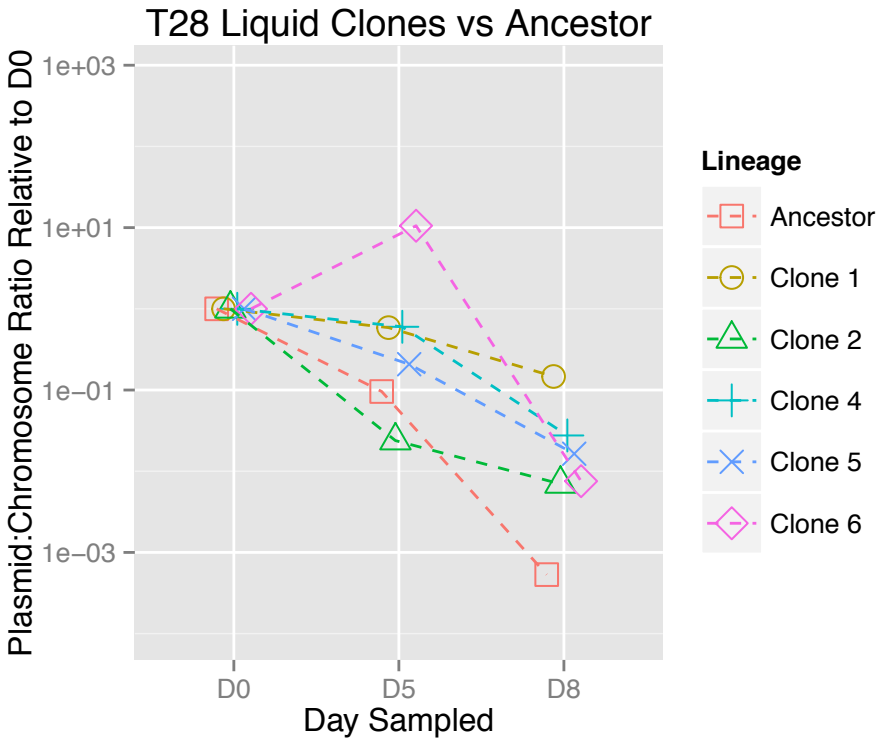

Figure 4. Plasmid stability in plasmid-host pairs from one T28 liquid replicate evolved in the presence of antibiotics. All pairs showed improvement over the ancestral state (DOD67; red box). Relatively consistent patterns of stability are seen across all clones; interestingly based on gel electrophoresis of extracted plasmid DNA and whole genome sequence analysis, pB10 derivatives in all clones showed large deletions similar to those in clones 5 and 6 of the T28 biofilm assays (Fig. 3; Task 3).

To determine if the observed improved plasmid stability is due to genetic changes in the host, the plasmid, or both, we extracted and purified the plasmid DNA from the 'evolved clones' (i.e. those clones that were the from the end-point of the evolution experiment) and transformed the plasmid DNA into the ancestral host (without pB10) by electroporation. These strain construction steps, have been successfully done for a few of the evolved biofilm clones and are underway for the remaining clones. Interestingly, we ran into some difficulty where full-length plasmids were being used (such as clones 1-4 in Fig. 3), as we were unable to successfully transform the ancestral host with them. Each time plasmid DNA from suspected transformants was analyzed, it showed large deletions, as seen in the other evolved clones. In parallel, sequence analysis (Task 3) showed that the *A. baumannii* host of the ancestral host-plasmid pair DOD67 has a deletion in a portion of their chromosome when compared to the ancestral host before pB10 was introduced. We then obtained a pB10-free segregant of *A. baumannii* from DOD67, and electroporation of this derivative strain with the deleted chromosomal region with evolved, full-length pB10 plasmids resulted in transformants with full-length plasmids. See Task 3 for more details on the deleted segment.

We have now successfully transformed this new *A. baumannii* strain with several of the plasmids from our biofilm-evolved clones (T28) for stability assays. Notably, the first results suggest that one of the evolved truncated plasmids (from clone 5 in Fig. 3) is much more stable than the ancestral pB10 in this host. Because no other mutations besides the deletion were detected on this evolved plasmid (see Task 3), these preliminary results suggest that for this truncated plasmid, the deleted segment in the plasmid can entirely explain the improved stability (see in Fig. 3). In contrast, one of the full-length plasmids from evolved clone 1 (Fig. 3) showed poor stability, similar to that of the ancestral plasmid. Together with the finding that this plasmid has undergone no mutations at all (see Task 3), this result suggests that the improved stability in the evolved clone are likely due to mutations in the host. Thus while preliminary, the observed diversity in stability patterns correlates with genotypic diversity (see Task 3 for details) that arose in the biofilms of *A. baumannii* within 28 days.

More work is required to complete the goals of this task. Namely, completion of the qPCR analysis of the sampled time point and culture is needed (e.g. other replicate populations at day T0 and T28, and some of the T14 samples for both liquid and biofilm evolution experiments). Further testing of plasmids derived from evolved clones in the ancestral host is underway.

C. Task 3

We have now completely sequenced 20 bacterial strains from this experiment to date: 6 clones from one biofilm replicate harvested at T0 (DOD321-326), 6 clones from one biofilm harvested at T28 (DOD357-362, clones 1-6 in Fig. 3 respectively), and 6 clones from one of the three populations in the liquid culture experiment (DOD393-398); the pB10-containing ancestor used to inoculate all biofilms (DOD67); and the rifampicin resistant *A. baumannii* strain (DOD 15) that was electroporated with pB10 to generate DOD67. To prepare for sequencing, DNA was extracted from a liquid culture grown from each colony; extracted DNAs were then sent to the University of Idaho Genomics Resource Core (UI GRC) for library preparation and sequencing. Sequencing was performed on the Illumina MiSeq platform and sequences were assembled using Assembly by Reduced Complexity (ARC).

Sequence data from pB10 were first mapped to a reference genome of pB10 obtained from GenBank to compare the plasmid sequence data across all samples (Fig. 5). We then aligned the assembled contigs for pB10 from each sample to a reference sequence obtained from GenBank and analyzed each to look for single nucleotide polymorphisms (SNPs) and examine deletions in detail. The pB10 plasmid found in our ancestor (DOD67), showed no SNPs when compared to the reference, and there was no evidence of any deletions (Fig. 5). This was also true for all 6 clones sequenced from the biofilm harvested at T0, and for 4 of the 6 clones sequenced from a T28 biofilm. The remaining two clones from the T28 biofilm showed two different, large, deletions of the region of pB10 that are responsible for conjugative plasmid transfer, but again no SNPs. All six clones that evolved in liquid cultures until day T28 shared another large deletion of the conjugation and transfer region of pB10 (Fig. 5).

Tying this information on deletions with the stability assays (Fig. 3) where high levels of plasmid stability were observed for clones 5 and 6 (DOD361, DOD362 in Fig. 4) points to

the fact that pB10 may have switched to a vertically transmitted life-history, because horizontal transfer genes have been eliminated. From an evolutionary standpoint, vertical transmission is desirable for *A. baumannii* in this environment with abundant antibiotics because it guarantees that all progeny will survive. However, loss of the ability to horizontally transfer to new hosts is a 'risky' strategy for the plasmid because it can no longer escape to other bacteria in any environment where its (now obligate) host is unfit. Of further interest is the fact that preliminary data from the stability of one truncated plasmids in the ancestral host suggest high stability as well (see Task 2), suggesting the observed deletions may be sufficient to produce stability in any *A. baumannii* genetic background. Finally, the fact that clone 3 from the T28 biofilm is stable (Fig. 3) but does not have the same deletions (Fig. 5) suggests that biofilms are indeed allowing for different, variable solutions to the presented evolutionary challenge, as hypothesized.

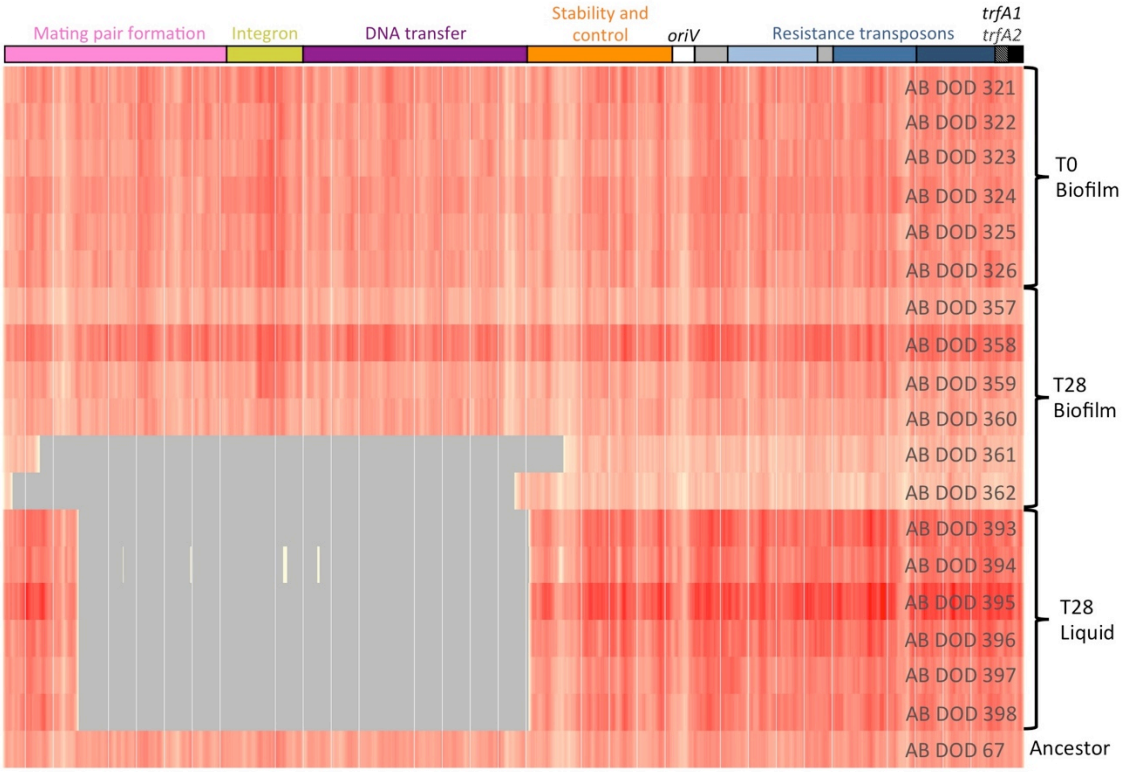

Figure 5: Heat map showing sequence data from pB10 for 19 samples. Red indicates how frequent a particular site is relative to the chromosomal DNA sequenced from the same sample (Bright red = 8 times as frequent, tan = same frequency as chromosomal DNA). Gray indicates sites that are missing from that sample. The map at the top shows the function of genes found within each region of the plasmid. The bar along the top of the heat map indicates the type of genes found with a region of the plasmid. The missing sites (i.e. putative deletions) are similar for all of the truncated plasmids and involve genes for plasmid transfer, the integron, and genes for mating pair formation.

Similar to the data from pB10, sequence data from the *A. baumannii* chromosome were first mapped to a reference genome of *A. baumannii* ATCC 17978 obtained from GenBank to compare the sequence data across all samples. This mapping showed that a large section of the host chromosome, roughly 124 kb, had been deleted between the isolation of the plasmid-free *A. baumannii* in DOD15 and isolation of pB10 containing *A. baumannii* in DOD67, which was used to seed our experiments (Fig. 6). The same deletion is present in all 18 sequenced strains that evolved from this ancestor (i.e. all those *A. baumannii* isolated from biofilms and liquid cultures). Additionally, sequence data from the previous version of this experiment (not shown) indicate that all previous pB10 containing samples of *A. baumannii* that we sequenced had either a loss of the same region, or loss of a smaller region containing a subset of the genes lost in the larger region. We are in the process of exploring which genes are present in this region in an attempt to explain why this deletion is associated with presence of the pB10 plasmid. As mentioned in the description of progress on Task 2, attempts at electroporation of full-length plasmids into *A. baumannii* still carrying this region (Fig. 5 DOD15) failed. We hypothesize that the deleted segment somehow did not allow establishment of the full-size plasmid. We do not understand the underlying mechanism for this phenomenon yet but preliminary automated annotation suggests that some of the deleted genes encode transposases, integrases, and some typical plasmid encoded genes like replication and a few transfer genes. We speculate that the deleted fragment contained a genomic island. Further analysis is required to explain this interesting phenomenon.

Since the improved stability of a few full-length unchanged pB10 plasmids cannot be explained by changes in the plasmid, there are likely to be chromosomal mutations that are responsible for improved plasmid persistence. Analyses of the chromosomal sequences of evolved clones to detect single nucleotide polymorphisms and insertions and deletions that may be responsible for this phenotype are underway. Chromosomal mutations in the host may be a likely mechanism for improved plasmid stability in environments where the cost of being plasmid free is high (such as growth in an antibiotic laden culture) and thus there is strong selection on the host to retain the plasmid.

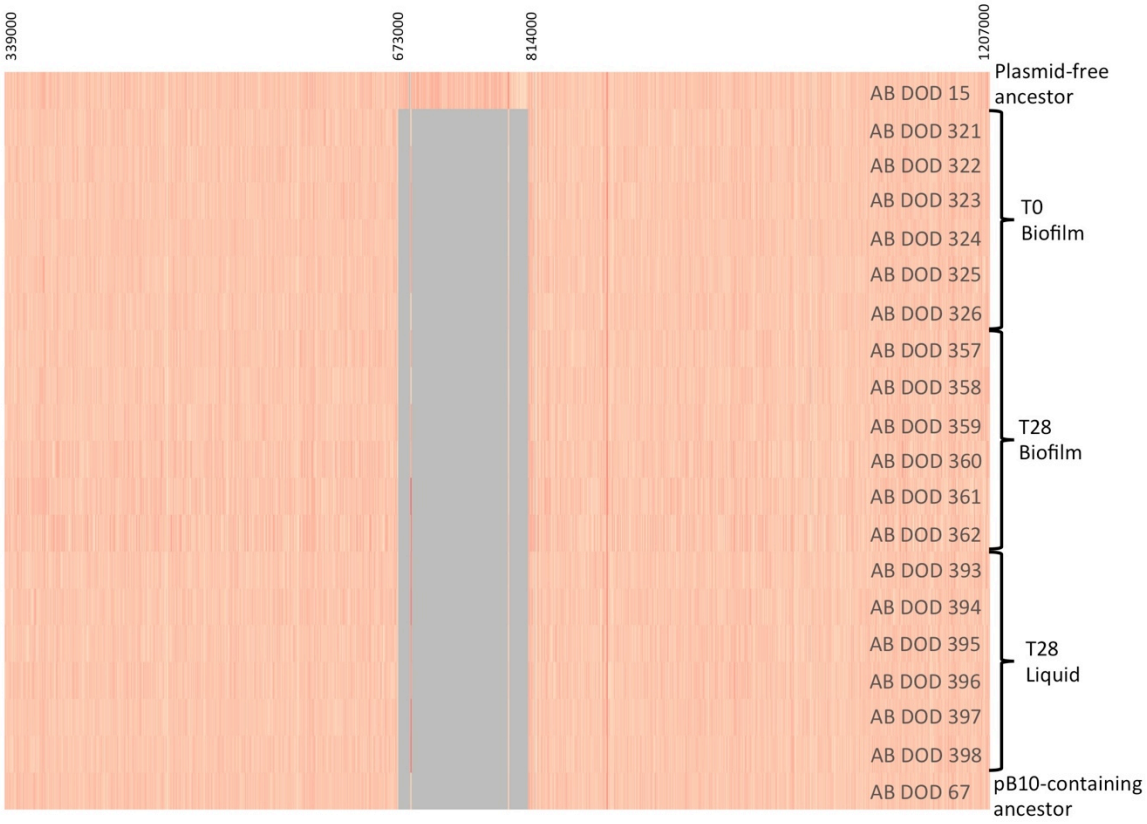

Figure 6. Heat map showing sequence data from *A. baumannii* for 20 strains: original A. baumannii host, the strain after introduction of plasmid pB10, and 18 clones evolved in biofilms and liquid cultures. The intensity of the red color correlates with the frequency of a particular site relative to other DNA sequences from the same genome (bright red are have a higher coverage while tan indicates fewer sequencing reads). Gray indicates sites that are missing from that genome. All 18 *A. baumannii* clones descending from DOD67 show the same pattern of deletion, as would be expected unless further deletions were accrued. Further analyses looking for single nucleotide polymorphisms and insertions/deletions in the chromosome are underway.

4. KEY RESEARCH ACCOMPLISHMENTS

We break down our key research accomplishment by quarter for Year 2 (Q5-8; months 13-24). It should be noted that some of the finding from Q5 and Q6 would require more testing, because of problems we experienced while performing the planned work (namely mutations associated with the artificially inserted *gfp* gene). These issues led to modifications of our experimental design (see Fig. 2 for new work scheme).

A. Fifth Quarter (Months 13-15)

1. The persistence of antibiotic resistance genes in *A. baumannii* (pB10::gfp) biofilms was much higher than in well-mixed liquid cultures, in spite of lack of antibiotic selection.
2. In biofilms, plasmid pB10::*gfp* seemed to have undergone deletions that removed the fluorescence phenotype but retained the resistance genes under study, even

in the absence of antibiotic selection pressure. Genome sequencing verified the molecular changes in these plasmids.

3. Another important finding was the drastic improvement of the persistence of plasmid pB10::*gfp* after evolving liquid cultures of host *A. baumannii* for 500 generations (50 days).

B. Sixth Quarter (Months 16-18)

1. Whole genome sequencing of 10 biofilm clones of pB10::*gfp* showed that deletions of various large plasmid segments occurred in different clones. This suggested that antibiotic resistance genes may have been retained better in biofilms than in mixed liquids via structural changes in the plasmid.
2. Evidence further highlighted that plasmid pB10::*gfp* significantly improved its persistence after evolution under antibiotic selection in liquid serial batch cultures for 50 days. Resequencing of evolved clones suggested large deletions in the plasmid as well as integration in the chromosome in some of the evolved lineages.
3. Loss of a functional *gfp* gene on pB10 (due to deletions and chromosomal integration) called into question whether structural changes in pB10 were due to the artificial insertion of the mini-transposon containing *gfp*.

C. Seventh Quarter (Months 19-20)

1. We started new evolution experiments with *Acinetobacter baumannii* ATCC 17978 and using the natural unmarked plasmid pB10 as a model multi-drug resistance plasmid, instead of the *gfp*-marked plasmid (pB10::*gfp*). The new design allows (Fig. 2) us to determine whether or not some of the observed drastic structural plasmid rearrangements are due to the artificial insertion of the mini-transposon containing *gfp*.
2. We found that the unmarked pB10 plasmid frequently undergoes deletions when transferred into *A. baumannii*, resulting in loss of most of the conjugative transfer and mating pair formation regions of the plasmid and thus rendering it non-self-transmissible (Fig. 4). This form of specialization of the broad-host-range plasmid pB10 to its host by losing its horizontal transfer capacity has not been previously observed in our many studies with other bacterial hosts.
3. Sequencing showed that a large segment of pB10::*gfp* plasmid had been integrated into the chromosome of clones from two of the five independently evolved lineages in liquid batch culture.

D. Eigth Quarter (Month 21-24)

1. We completed the growth of replicated liquid and biofilm cultures in the presence antibiotics for 28 days.
2. Procedures for DNA extraction using the QIASymphony robot and subsequent qPCR using the *trfA* gene of pB10 and the 16S rRNA gene of *A. baumannii* were developed and optimized (this was necessary due to the use of the unmarked

pB10 plasmid). We created a data analysis pipeline for the incoming qPCR data using the R statistical programming language.

3. Stability analyses of the T28 biofilm culture show elevated levels of pB10 persistence. Genetic analysis (using sequencing and gel electrophoresis) however has demonstrated that fundamentally different mechanisms maintaining a plasmid have arisen; specifically, some high-stability clones show deletions of large portion of the plasmid while others do not (Fig. 3-5).
4. Sequencing of plasmid from the T28 liquid culture show identical deletions in all six clones from one replicate (Fig. 4). Together with point 3, these findings support our hypothesis that biofilm growth allows coexistence of multiple genotypes and thus higher diversity than that after evolution in liquids. Two more replicate biofilm and liquid cultures remain to be analyzed however.
5. Preliminary data show greatly improved stability of plasmid pB10 evolved in biofilms in the ancestral host. These findings are consistent with the hypothesis that the genetic changes responsible for increased stability are encoded on the evolved, smaller versions of pB10 and do not depend on the host genetic background. Thus in some cases deletion of the transfer genes can explain improved plasmid persistence. These results strongly suggest that plasmid-encoded antibiotic resistance can be retained in *A. baumannii* by deletion of the conjugative transfer genes, thus restricting the host range of the plasmid to this one host as well as drastically decreasing the fitness cost of harboring the plasmid.
6. Interestingly, we found evidence that the deletion that occurred in *A. baumannii* upon introduction of plasmid pB10 may be necessary for *A. baumannii* to host a full-length pB10 plasmid. This is a very interesting observation and will be examined further in the next quarter. It suggests that under selection for an incoming drug resistance plasmid, this opportunistic pathogen can eliminate a negative interaction between one of its chromosomal segments and the plasmid by simply deleting the appropriate chromosomal segment.
7. None of the sequenced *A. baumannii* clones show any structural changes compared to the ancestral host with pB10 (DOD67; Fig. 5). Identification of smaller changes, such as single nucleotide polymorphisms and small insertions/deletions requires further study.

5. CONCLUSIONS

Nosocomial infections of combat wounds in military treatment facilities in the US have become a major problem, and are commonly caused by MDR Gram-negative bacteria such as *P. aeruginosa, A. baumannii, K. pneumoniae, Enterobacter sp.* and *E. coli* (Eardly *et al.*, 2011). In particular, *A. baumannii* which we are studying is an important pathogen responsible for outbreaks of nosocomial infections in intensive care units, including those in military hospitals (Adams-Haduch *et al.*, 2008; Dijkshoorn *et al.*, 2007; Gaynes *et al.*, 2005; Peleg *et al.*, 2008). Strains of these species are often resistant to multiple antibiotics as a result of genes encoded on so-called multi-drug resistance (MDR) plasmids they carry. This wide-spread resistance to antimicrobial agents has lead to decreasing effectiveness of current antibiotic treatments, so much that the CDC recently declared antimicrobial

resistance as "one of our most serious health threats". Moreover, the bacteria in these wounds often grow in biofilms, which are considered 'hot-spots' for plasmid transfer. However, the adaptive mechanisms by which MDR plasmids are able to persist in bacterial populations even in the absence of antibiotics remains poorly understood. Our main goal of this project is to understand how MDR broad-host-range plasmids can become more stable (i.e. persist) in important wound pathogens like *A. baumannii*, thus perpetuating their encoded resistance traits. We postulated that the spatial structure of biofilms affects the persistence of MDR plasmids, as well as the evolutionary pathways that further improve that persistence. **We now have preliminary evidence that this is case; we have found that multiple strategies to increased plasmid stability have evolved in biofilms (Figs. 3,5), while liquid cultures led to what seems to be a single strategy for maintaining antibiotic resistance (see pB10 plasmid sequences from DOD393-398 in Fig. 5).**

Our current results indicate that **the structured biofilm environment, which typically characterizes the type of bacterial growth in wounds, facilitates the persistence of MDR plasmids**. Moreover, we have indications that **changes in the *A. baumannii* host (Fig. 6) are required for uptake of full-length pB10 plasmids and that pB10 commonly undergoes truncation to a variant that is likely to only be vertically transmitted.** While still partially uncharacterized, these genetic modifications likely decrease plasmid cost to the host while increasing the retention of favorable plasmid-encoded traits (i.e. antibiotic resistance). Once these structural changes and other possible mutations are characterized through further analysis in Year 3, this project has already greatly contributed to our understanding of the pathways through which stable plasmid persistence is achieved in wound-like biofilm environments.

The fundamental insights obtained so far will support future research into novel drug therapies that are based on restricting the dissemination and stable replication of MDR plasmids. Such therapies have recently been proposed by others in the field and are rapidly gaining interest given the alarmingly growing ineffectiveness of currently used antibiotics (Baquero *et al.*, 2011; Lujan *et al.* 2007; Williams *et al.*, 2011). Rather than trying to kill the bacteria, these new compounds aim at preventing the emergence of bacteria resistant to the next generation of antibiotics, by inhibiting spread and stable persistence of the mobile elements that carry the corresponding resistance genes. They will ultimately be useful in the care of patients with trauma-induced wounds, and may thus have a significant impact on the mortality rates of wounded troops as well as their ability to return to combat after injury (Eardly *et al.*, 2011).

6. PUBLICATIONS, ABSTRACTS, AND PRESENTATIONS

A. Manuscripts

- Loftie-Eaton, W., A. Tucker, A. Norton, and E.M. Top. 2014. Flow cytometry and Real-Time qPCR as tools for assessing plasmid stability. Appl. Environ. Microbiol. 80(17):5439.

B. Presentations

1. *Oral presentations*:

- Top, E.M. Rapidly improving persistence of multi-drug resistance plasmids in well-mixed populations and spatially structured biofilms. International Society for

Plasmid Biology meeting (ISPB). Palm Cove, Australia, October 27-November 1, 2014.

- Top, E.M. The plasticity of plasmid host range. "The History of Plasmids". Cold Spring Harbor Laboratory, Long Island, New York, September 21-24.

2. *Posters*:

- Regmi R, Smith SE, Millstein JH, Cornea A, France MT, Corona Hernandez D, Forney LJ, Top EM. 2013. Effects of spatial structure on the co-evolution of multi-drug resistance plasmids and their host. Poster presented at the 2013 IBEST Science Expo, University of Idaho, Moscow, ID, October 18, 2013.
- Regmi R, Smith SE, Millstein JH, Cornea A, France MT, Corona Hernandez D, Forney LJ, Top EM. 2013. Effects of spatial structure on the co-evolution of multi-drug resistance plasmids and their host. Poster presented at the College of Science Student Research Exposition, University of Idaho, Moscow, ID, November 8, 2013.
- Regmi R, Avery RA, Millstein JH, Smith SE, and Top EM. Effects of Antibiotic Selection on the Page 17 of 23Persistence of multi-drug resistance plasmids in *Acinetobacter baumannii.*. University of Idaho Innovation Showcase, April 16, 2014.
- Regmi R, Avery RA, Millstein JH, Smith SE, and Top EM. Effects of antibiotic selection on the persistence of multi-drug resistance plasmids in *Acinetobacter baumannii.* Biological Sciences Undergraduate Research Symposium, University of Idaho, May 7, 2014.
- Metzger, GA, Smith, SE, Stalder, T, Gliniewicz, K, Settles, M, Millstein, J, Forney, LJ, Top, EM. Maintenance of plasmid-encoded drug resistance in *Acinetobacter baumannii* in liquid culture and biofilms. Evolution, June 22, 2014.
- Metzger, GA, Millstein, JH, Stalder, T, Gliniewicz, K, Settles, M, Ridenhour, BJ, Forney, LJ, and Top, EM. Maintenance of plasmid-encoded drug resistance in *Acinetobacter baumannii* in liquid culture and biofilms. 10th Annual College of Science Student Research Expo, University of Idaho. October 17, 2014. **Winner of Best Graduate Student Poster**.

7. INVENTIONS, PATENTS, AND LICENSES

None to report.

8. REPORTABLE OUTCOMES

See 6.A. Manuscripts.

9. OTHER ACHIEVEMENTS

None to report.

10. REFERENCES

Adams-Haduch, J. M., D. L. Paterson, H. E. Sidjabat, A. W. Pasculle, B. A. Potoski, C. A. Muto, L. H. Harrison, and Y. Doi. 2008. Genetic basis of multidrug resistance in *Acinetobacter baumannii* clinical Isolates at a tertiary medical center in Pennsylvania. Antimicrob. Agents Chemother. 52:3837-3843.

Baquero, F., T. M. Coque, and F. de la Cruz. 2011. Ecology and evolution as targets: the need for novel eco-evo drugs and strategies to fight antibiotic resistance. Antimicrob. Agents Chemother. 55:3649-3660.

Center for Disease Control and Prevention (CDC), US Department of Health and Human Services. Antibiotic resistance threats in the United States, 2013.

Dijkshoorn, L., A. Nemec, and H. Seifert. 2007. An increasing threat in hospitals: multidrug-resistant *Acinetobacter baumannii*. Nat. Rev. Microbiol. 5:939-951.

Eardley, W. G. P., K. V. Brown, T. J. Bonner, A. D. Green, and J. C. Clasper. 2011. Infection in conflict wounded. Phil. Trans. R. Soc. Lon. B. 366:204-218.

Gaynes, R., and J. R. Edwards. 2005. Overview of nosocomial infections caused by gram-negative bacilli. Clin. Infect. Dis. 41:848-854.

Loftie-Eaton, W., A. Tucker, A. Norton, and E.M. Top. 2014. Flow cytometry and Real-Time qPCR as tools for assessing plasmid stability. Appl. Environ. Microbiol. 80:5439-5446.

Lujan, S. A., L. M. Guogas, H. Ragonese, S. W. Matson, and M. R. Redinbo. 2007. Disrupting antibiotic resistance propagation by inhibiting the conjugative DNA relaxase. Proc. Natl. Acad. Sci. U. S. A. 104:12282-12287.

Murray, C. K. 2008. Infectious disease complications of combat-related injuries. Crit. Care Med. 36:S358-S364.

Peleg, A. Y., H. Seifert, and D. L. Paterson. 2008. *Acinetobacter baumannii*: Emergence of a successful pathogen. Clin. Microbiol. Rev. 21:538-582.

Schlüter, A., H. Heuer, R. Szczepanowski, L. J. Forney, C. M. Thomas, A. Pühler, and E. M. Top. 2003. The 64,508 bp IncP-1β antibiotic multiresistance plasmid pB10 isolated from a waste-water treatment plant provides evidence for recombination between members of different branches of the IncP-1beta group. Microbiology 149:3139-3153.

Williams, J. J., E. M. Halvorsen, E. M. Dwyer, R. M. DiFazio, and P. J. Hergenrother. 2011. Toxin-antitoxin (TA) systems are prevalent and transcribed in clinical isolates of *Pseudomonas aeruginosa* and methicillin-resistant *Staphylococcus aureus.* FEMS Microbiol. Lett. 322:41-50.

11. APPENDICES

A. R script for qPCR data

The following script reads in and analyzes raw data file from an Applied Biosystems real-PCR machine. Example data files are in section B. The analysis calculates starting concentrations of the trfA plasmid gene and 16S bacterial gene on a well-by-well basis using estimation of logistic growth curves. Parametric bootstraps of the estimated initial concentration are returned for plotting and statistical testing.

```
#functions & libraries
library(MASS)
library(boot)
library(ggplot2)
```

```
library(xlsx)

timeShift<-function(inData){
  out<-
data.frame(Well=character(0),Cycle=numeric(0),x=numeric(0),y=numeric(0))
  currEnv<-environment()
  with(inData,{
    for(w in unique(Well)){
      sub<-Well==w
      len.sub<-sum(sub)
      cyc<-Cycle[sub]
      cyc<-cyc[1:(len.sub-1)]
      vals<-X_Rn[sub]
      x<-vals[1:(len.sub-1)]
      y<-vals[2:len.sub]
      assign("out",rbind(out,data.frame(Well=w,Cycle=cyc,x,y)),envir=currEnv)
    }
  }
  )
  out
}

use2wells<-function(inData){
  wells<-unique(inData$Well)
  if(length(wells)<=2) return(inData)
  wellData<-data.frame(Cycle=1:max(inData$Cycle))
  for(w in wells){
    temp<-inData[inData$Well==w,c("Cycle","X_Rn")]
    names(temp)<-c("Cycle",w)
    wellData<-merge(wellData,temp,by=c("Cycle"),all.x=TRUE)
  }
  corMatrix<-cor(wellData,use="pairwise.complete.obs")
  corMatrix[lower.tri(corMatrix,diag=TRUE)]<-NA
  indices<-which(corMatrix==max(corMatrix,na.rm=T),arr.ind=TRUE)
  inData[inData$Well %in% rownames(corMatrix)[indices],]
}

#general logistic equation
logisticF<-function(n0,data,r,k) n0*exp(r*data$Cycle)*k/(k-
n0+exp(r*data$Cycle)*n0)

#calculate the sums of squares
optn0<-function(n0,data,r,k) sum((data$X_Rn - logisticF(n0,data,r,k))^2)

#minimize sums of squares to find n0
bootOpt<-function(params,pcrData){
  optimize(optn0,c(0,1),pcrData,params[1],-
params[1]/params[2],tol=.Machine$double.eps)$minimum
}

#workhorse function, use the flags for ratio, rna, and trf to control
#which samples are analyzed (ratio = both, rna = 16S, trf = trf A)
findRatio<-function(pcrData,sampleName,ratio=TRUE,rna=FALSE,trf=FALSE){
  trfLabel<-paste("trfA_",sampleName,sep="")
  rnaLabel<-paste("16S rRNA gene_",sampleName,sep="")
  sample1 <-use2wells(pcrData[pcrData$sample==rnaLabel,])
  sample2 <-use2wells(pcrData[pcrData$sample==trfLabel,])
```

```
  if(nrow(sample1)==0 && (ratio || rna)) stop("No sample data available for
",rnaLabel)
  if(nrow(sample2)==0 && (ratio || trf)) stop("No sample data available for
",trfLabel)

  rnaData<-timeShift(sample1)
  trfData<-timeShift(sample2)

  sample1<-na.omit(sample1)
  sample2<-na.omit(sample2)

  rnaModel<-glm(y~x+I(x^2)-1+offset(x),data=rnaData)
  trfModel<-glm(y~x+I(x^2)-1+offset(x),data=trfData)

  if(ratio || rna) rnaBoot<-
boot(coef(rnaModel),bootOpt,1000,sim="parametric",pcrData=sample1,ran.gen=fun
ction(mu,sigma) mvrnorm(1,mu,sigma),mle=vcov(rnaModel))
  if(ratio || trf) trfBoot<-
boot(coef(trfModel),bootOpt,1000,sim="parametric",pcrData=sample2,ran.gen=fun
ction(mu,sigma) mvrnorm(1,mu,sigma),mle=vcov(trfModel))

  out<-list()
  if(ratio){out$t0<-trfBoot$t0/rnaBoot$t0; out$t<-trfBoot$t/rnaBoot$t}
  if(rna){out$rna_t0<-rnaBoot$t0; out$rna_t<-rnaBoot$t}
  if(trf){out$trf_t0<-trfBoot$t0; out$trf_t<-trfBoot$t}
  out
}

#read in data from files & clean, writes data to global env
getData<-function(x){
  fn<-1
  for(i in x){
    sampleNames<-read.xlsx2(i,sheetName="Sample
Setup",startRow=8,colIndex=1:11,header=T)
    pcrData<-read.xlsx2(i,sheetName="Amplification
Data",startRow=8,colIndex=1:5,header=T,colClass=c("character","numeric","char
acter","numeric","numeric"))

    names(pcrData)[5]<-"X_Rn"
    #pcrData$Cycle<-as.numeric(pcrData$Cycle)
    #pcrData$Rn<-as.numeric(pcrData$Rn)
    #pcrData$X_Rn<-as.numeric(pcrData$X_Rn)

    pcrData<-na.omit(pcrData)
    sampleNames$sample<-
paste(sampleNames$Target.Name,"_",sampleNames$Sample.Name,sep="")

    pcrData<-merge(pcrData,sampleNames[,c("Well","sample")])

    pcrData$X_Rn[pcrData$X_Rn <= 0]<-NA
    #this one drops wells where by the last cycle the fluorescence did not
exceed 1
    pcrData<-pcrData[! pcrData$Well %in% pcrData[pcrData$Cycle ==
max(pcrData$Cycle) & pcrData$X_Rn < 1,"Well"], ]

    assign(paste("qPCRx",fn,sep=""),pcrData,envir=.GlobalEnv)

    fn<-fn+1
```

```
  }
}

#analyze data in one fell swoop, x is a vector of file names
# "..." passes arguments to find ratio
analyzeQPCR<-
function(x,samps=c("t0","t1","t2","t3","t4","t5","t6","t7","t8","t9"),prefix=
"ratio",...){
  getData(x)
  #i indexes the input file, j indexes the sample identify (e.g. t0, t1)
  for(i in 1:length(x)){
    for(j in samps){

try(assign(paste(prefix,"_",j,"_rep",i,sep=""),findRatio(get(paste("qPCRx",i,
sep="")),j,...),envir=.GlobalEnv))
    }
  }
}

#easy collation of bootstraps
collate<-function(x,lastcol=FALSE,lastName="ID",lastVal=NULL){
  out  <- data.frame(Sample=character(0),Estimates=numeric(0))
  for(i in x) out<-rbind(out,data.frame(Sample=i,Estimates=get(i)$t))
  if(lastcol) out[,lastName]<-lastVal
  out
}

#### this is to be run on collated data sets
makeRelative<-function(x){
  days<-sub("t","D",sub("^ratio_","",sub("_rep.$","",x$Sample)))
  baselines<-x$Estimates[days=="D0"]
  if(!length(baselines)) stop("No data were present for day 0. Aborting.")
  out<-x[0,1:2]
  for(i in unique(days)){
    if(i=="D0") next
    out<-rbind(out,data.frame(i,x$Estimates[days==i]/baselines))
  }
  if(ncol(x) == 3) out[,3]<-x[1,3]
  names(out)<-names(x)
  out
}

multiplot <- function(..., plotlist=NULL, file, cols=1, layout=NULL) {
  require(grid)

  # Make a list from the ... arguments and plotlist
  plots <- c(list(...), plotlist)

  numPlots = length(plots)

  # If layout is NULL, then use 'cols' to determine layout
  if (is.null(layout)) {
    # Make the panel
    # ncol: Number of columns of plots
    # nrow: Number of rows needed, calculated from # of cols
    layout <- matrix(seq(1, cols * ceiling(numPlots/cols)),
                     ncol = cols, nrow = ceiling(numPlots/cols))
  }
```

```
  if (numPlots==1) {
    print(plots[[1]])

  } else {
    # Set up the page
    grid.newpage()
    pushViewport(viewport(layout = grid.layout(nrow(layout), ncol(layout))))

    # Make each plot, in the correct location
    for (i in 1:numPlots) {
      # Get the i,j matrix positions of the regions that contain this subplot
      matchidx <- as.data.frame(which(layout == i, arr.ind = TRUE))

      print(plots[[i]], vp = viewport(layout.pos.row = matchidx$row,
                                      layout.pos.col = matchidx$col))
    }
  }
}
```

B. Sample Data

The R script in Appendix A read *.xls/*.xlsx formatted data. Two worksheets get read; these worksheets are labeled “Sample Setup” and “Amplification Data”.

The “Sample Setup” worksheet layout should be as follows (only wells A1-A7 shown):

Block Type	96well
Chemistry	SYBR_GREEN
Experiment File Name	C:\Documents and Settings\INSTR-ADMIN\Desktop\Forney Lab\Top Lab Projects\2014-10-21 DOD397-398 t0-t5-t8 assays.eds
Experiment Run End Time	Not Started
Instrument Type	steponeplus
Passive Reference	ROX

Well	Sample Name	Sample Color	Biogroup Name	Biogroup Color	Target Name	Target Color	Task	Reporter	Quencher	Quantity	Comments
A1	2ng	RGB(132,193,241)			16S rRNA gene	RGB(139,189,249)	STANDARD	SYBR	None	2	
A2	2ng	RGB(132,193,241)			16S rRNA gene	RGB(139,189,249)	STANDARD	SYBR	None	2	
A3	2ng	RGB(132,193,241)			16S rRNA gene	RGB(139,189,249)	STANDARD	SYBR	None	2	
A4	0.2ng	RGB(168,255,222)			16S rRNA gene	RGB(139,189,249)	STANDARD	SYBR	None	0.2	
A5	0.2ng	RGB(168,255,222)			16S rRNA gene	RGB(139,189,249)	STANDARD	SYBR	None	0.2	
A6	0.2ng	RGB(168,255,222)			16S rRNA gene	RGB(139,189,249)	STANDARD	SYBR	None	0.2	
A7	0.02ng	RGB(223,221,142)			16S rRNA gene	RGB(139,189,249)	STANDARD	SYBR	None	0.02	

The script reads the “Well”, “Sample Name” and “Target Name” columns from this worksheet to identify samples that were tested and the gene target for a particular well.

The “Amplification Data” worksheet layout should be (only cycles 1-7 for A1 shown):

Block Type	96well
Chemistry	SYBR_GREEN
Experiment	C:\Documents and Settings\INSTR-ADMIN\Desktop\F
Experiment	Not Started
Instrument	steponeplus
Passive Re	ROX

Well	Cycle	Target Name	Rn	ΔRn
A1	1	16S rRNA gene	-0.03922	-0.02789
A1	2	16S rRNA gene	-0.01092	-0.00955
A1	3	16S rRNA gene	0.006644	-0.00196
A1	4	16S rRNA gene	0.020441	0.001872
A1	5	16S rRNA gene	0.029943	0.001407
A1	6	16S rRNA gene	0.037907	-0.0006
A1	7	16S rRNA gene	0.047747	-0.00072

The script reads the "Well", "Cycle", and "ΔRn" columns. Well numbers are then matched against the metadata collected from the "Sample Setup" worksheet.

C. Example qPCR analysis with R

Utilizing the script provided in Appendix A with data formatted like that in Appendix B can be analyzed in the following manner using R. We assume that the script Appendix A is saved as "script.R" and two data files, "data1.xls" and "data2.xls", are all present in the directory "/home/user/Desktop". We want to analyze data for samples named "S1" and "S2" (so named in the "Sample Setup" worksheet).

```
setwd("/home/user/Desktop") #change to the appropriate directory
source("script.R") #read script file to get analysis functions
#launch the analysis on the files and samples
analyzeQPCR(c("data1.xls","data2.xls"), samps=c("S1","S2"))

#assemble analysis output into two data frames
#lastVal determines the identifier to give output from a particular file
#e.g. here everything from "data1.xls" will have identifier of "Rep1"
r1<-collate(ls(patt="*rep1"),TRUE,lastVal="Rep1")
r2<-collate(ls(patt="*rep2"),TRUE,lastVal="Rep2")

#merge the data from the two files
allOutput<-rbind(r1,r2)

#at this point allOutput can be used for plotting stability curves
#or determining properties such as the mean and variance for plasmid
#stability on a given day
```

D. Published Paper Reprints

Flow Cytometry and Real-Time Quantitative PCR as Tools for Assessing Plasmid Persistence

Wesley Loftie-Eaton, Allison Tucker, Ann Norton and Eva M. Top

Appl. Environ. Microbiol. **2014, 80(17):5439. DOI: 10.1128/AEM.00793-14.**
Published Ahead of Print 27 June 2014.

AEM
Journals.ASM.org

Flow Cytometry and Real-Time Quantitative PCR as Tools for Assessing Plasmid Persistence

Wesley Loftie-Eaton,[a,b] Allison Tucker,[b,c,d] Ann Norton,[b] Eva M. Top[a,b,c]

Department of Biological Sciences,[a] Institute for Bioinformatics and Evolutionary Studies (IBEST),[b] Bioinformatics and Computational Biology Program,[c] and Departments of Mathematics and Statistics,[d] University of Idaho, Moscow, Idaho, USA

The maintenance of a plasmid in the absence of selection for plasmid-borne genes is not guaranteed. However, plasmid persistence can evolve under selective conditions. Studying the molecular mechanisms behind the evolution of plasmid persistence is key to understanding how plasmids are maintained under nonselective conditions. Given the current crisis of rapid antibiotic resistance spread by multidrug resistance plasmids, this insight is of high medical relevance. The conventional method for monitoring plasmid persistence (i.e., the fraction of plasmid-containing cells in a population over time) is based on cultivation and involves differentiating colonies of plasmid-containing and plasmid-free cells on agar plates. However, this technique is time-consuming and does not easily lend itself to high-throughput applications. Here, we present flow cytometry (FCM) and real-time quantitative PCR (qPCR) as alternative tools for monitoring plasmid persistence. For this, we measured the persistence of a model plasmid, pB10::*gfp*, in three *Pseudomonas* hosts and in known mixtures of plasmid-containing and -free cells. We also compared three performance criteria: dynamic range, resolution, and variance. Although not without exceptions, both techniques generated estimates of overall plasmid loss rates that were rather similar to those generated by the conventional plate count (PC) method. They also were able to resolve differences in loss rates between artificial plasmid persistence assays. Finally, we briefly discuss the advantages and disadvantages for each technique and conclude that, overall, both FCM and real-time qPCR are suitable alternatives to cultivation-based methods for routine measurement of plasmid persistence, thereby opening avenues for high-throughput analyses.

Many bacterial plasmids carry genetic information required for maintaining themselves in their prokaryotic host populations (1). The ability of a plasmid to persist in a growing bacterial population in the absence of selection typically is referred to as high plasmid stability; here, it is referred to as plasmid persistence. In addition to the replication initiator and one or more origins of replication, functions to ensure plasmid persistence can include multimer resolution, partitioning, postsegregational killing (toxin-antitoxin), and horizontal transfer systems (1, 2). In the absence of selection for the plasmid, plasmid persistence also is negatively affected by its cost to host fitness. Thus, plasmid persistence is a first indicator of how well a plasmid is adapted to that host. This can be useful to understand the natural long-term host range of a plasmid, determine its adaptation to novel hosts following experimental evolution in the laboratory, or identify useful plasmid vectors for biotechnological processes (3–7). From a human health perspective, understanding the evolution of plasmid persistence is critical if we are to manage the current crisis of rapid plasmid-mediated spread of antibiotic resistance (8, 9). Such studies are becoming increasingly demanding as we address more complex plasmid persistence questions involving multiple plasmids (10), hosts (4), and whole microbial communities (11). Therefore, efficient techniques for routine monitoring and quantification of plasmid persistence are much needed to facilitate progress in this field.

The ability of a plasmid to persist in a host typically is monitored (under laboratory conditions) by measuring the fraction of plasmid-containing cells within a bacterial population over time in serial batch cultures in the absence of positive selection for the plasmid. Conventionally this is achieved through cultivation-based methods in which diluted bacterial suspensions are spread on media with and without selection for plasmid-bearing cells or by replicating bacterial colonies (e.g., 50 or 100) from nonselective plates onto plasmid-selective and nonselective agar plates (4, 5, 12–17). However, this is labor-intensive, requires colony growth on agar, and has a built-in lag period of one or more days prior to knowing the results.

In recent years, researchers have successfully used alternative technologies, such as microscopy (cultivation dependent), FCM (flow cytometry), and real-time quantitative PCR (qPCR; both cultivation independent) to directly measure plasmid loss or to monitor the persistence of a plasmid in a bacterial population (11, 18–23). The microscopy-based techniques rely on monitoring the growth of single cells into microcolonies while directly observing the frequency with which plasmid-free cells are generated (18, 19). Although very advantageous for accurately measuring plasmid loss rates without the confounding effects of cost, this approach as currently described is not easily adapted to measuring the persistence of one or more plasmids in multiple hosts or in complex microbial communities. In contrast, Bahl et al. (20, 21) and Bonot and Merlin (11) demonstrated the versatility of FCM and real-time qPCR for this purpose by using these technologies to monitor plasmid persistence in bacteria within the gastrointestinal tract

Received 10 March 2014 **Accepted** 18 June 2014
Published ahead of print 27 June 2014
Editor: S.-J. Liu
Address correspondence to Eva M. Top, evatop@uidaho.edu.
Supplemental material for this article may be found at http://dx.doi.org/10.1128/AEM.00793-14.

doi:10.1128/AEM.00793-14

of rats and in sediment microcosms, respectively. They used the presence/absence of green fluorescence encoded by the *gfp* gene to distinguish plasmid-containing from plasmid-free cells by FCM or plasmid- and chromosome-specific real-time qPCR primers and probes to monitor the plasmid/chromosomal DNA ratio in microbial communities as a proxy for plasmid persistence and spread. However, specific development and demonstration of FCM and real-time qPCR for the purposes of routine quantification of plasmid persistence still is lacking.

Here, we rigorously compare and contrast the use of FCM and real-time qPCR as alternatives to conventional plating methods for routine measurement of plasmid persistence. We demonstrate the strengths and limitations of the methods by statistically comparing performance criteria, such as resolution, variance, and dynamic range, in plasmid persistence assays. This was done using a *gfp*-marked variant of the natural multidrug resistance plasmid pB10 and three different hosts wherein the wild-type plasmid previously has been shown to be stable, moderately unstable, and highly unstable (4).

MATERIALS AND METHODS

Bacterial strains, plasmids, and growth conditions. Plasmid pB10 was previously tagged with mini-Tn*5*-$P_{A1-04/03}$::*gfp*, a Tn*5* derivative transposon encoding green fluorescent protein (GFP) to produce pB10::*gfp* (24). The persistence of pB10::*gfp* was determined in *Pseudomonas putida* H2 (15), *P. putida* UWC-1 (25), and *P. veronii* S34 (26). To monitor plasmid persistence in so-called plasmid stability assays, here named plasmid persistence assays, all strains were cultured in Luria-Bertani (LB) broth at 30°C with shaking. Each day for the duration of the assays, 4.9 μl of culture was transferred into 5 ml of fresh media and incubated for 24 h, yielding ~10 generations per day. Kanamycin (50 μg/ml) and tetracycline (10 μg/ml) were added only to the precultures to try to ensure 100% plasmid retention at the start of the persistence assays (T_0). The cells harvested after each 24-h growth period were examined by the three methods. To set up mixed cultures with known ratios of plasmid-containing and plasmid-free *P. putida* UWC-1 cells, the optical density at 600 nm (OD_{600}) of each culture was standardized to 2.4, and the plasmid-containing cultures were diluted into the plasmid-free cultures following a 1:2, 1:3, or 1:10 dilution series, each spanning 6 dilution intervals.

General DNA techniques. Plasmid preparation, restriction endonuclease digestion, gel electrophoresis, and cloning were carried out using standard techniques (27, 28). DNA regions for cloning were amplified by PCR using 2× PCR master mix (Thermo Scientific) per the manufacturer's instructions. The reaction parameters included an initial denaturation step of 10 min at 94°C, 30 cycles of denaturation (30 s at 94°C), a variable annealing step dependent upon the average primer annealing temperature, and an elongation step at 72°C with the extension time dependent on the amplicon size.

Plate count assays. Each day for the duration of the persistence assays, dilutions of each culture were spread onto nonselective LB agar such that approximately 100 to 300 individual colonies were obtained per sample. The fraction of plasmid-containing colonies within each sampled population was determined by counting the fluorescent and nonfluorescent colonies during exposure to a 488-nm light source. To avoid the bias that would have been introduced due to the visible presence of GFP in plasmid-containing cells, the presence/absence of fluorescence was used as an indicator of plasmid presence/absence rather than antibiotic resistance, as is more commonly done (4, 5, 13–16).

Flow cytometry. In preparation for FCM analysis, 1 ml of each culture was centrifuged (8,000 rpm; 2 min), the supernatant discarded, and the cells resuspended in 1 ml phosphate-buffered saline (PBS; pH 7.4). The washed cells were diluted 10-fold in PBS, and 10^5 events (i.e., cells) were interrogated following exposure to a 488-nm light source using a BD FACSAria flow cytometer. The forward (FSC) and side scatter (SSC) photomultiplier voltages were set each day using a positive (plasmid-containing) and negative (plasmid-free) control for each strain such that both populations were optimally counted at a flow rate of 1,000 to 2,000 events per second. The SSC, FSC, and fluorescein isothiocyanate (FITC) photomultiplier voltages used for *P. putida* H2, *P. putida* UWC-1, and *P. veronii* S34 were 475 nV (SSC and FSC) and 675 nV (FITC); varying over time (days) between 350 to 500 nV (SSC and FSC) and 575 to 650 nV (FITC); and 450 nV (SSC), 425 nV (FSC), and 600 nV (FITC). The bacterial populations first were gated based on their SSC and FSC profiles to eliminate background events, which were recognized by sampling a blank PBS solution in parallel. Fluorescent and nonfluorescent cells within the gated population were discriminated based on fluorescent intensity (FITC-A). The FITC-A gate was set each day such that 99.5% of the positive-control population for each strain was counted as FITC-A positive (fluorescent). The BD FACSAria software (BD FACSDiva, firmware version 1.9) was used for data acquisition, and FlowJo v10 software was used for subsequent analysis.

Real-time qPCR. In the preparation of real-time qPCR, cell pellets collected after centrifugation (8,000 rpm for 2 min) of 0.5 ml per culture at each time point were stored at −20°C until total genomic DNA (gDNA) of all samples was extracted in a randomized order at the end of the 10-day assay using a Genelute bacterial gDNA kit (Sigma-Aldrich). The purified gDNA was quantified using a NanoDrop spectrophotometer. All real-time qPCRs were performed using a StepOnePlus real-time PCR system together with a Power SYBR green PCR master mix kit (Applied Biosystems) per the manufacturer's instructions. The amplification parameters for all real-time qPCRs were 94°C for 10 min, 40 cycles of 94°C for 15 s, and 60°C for 60 s. The melting curve parameters were 94°C for 15 s and 60°C for 30 s, followed by a temperature increase to 94°C with a ramp rate of 0.1%. The fluorescent signal was acquired after each 60°C amplification step and continuously during the melting curve analysis. Unless otherwise stated, 2 ng of template DNA was used per reaction.

For all three bacterial strains, the chromosomal DNA was quantified using the gammaproteobacterium-specific qPCR primers 1080γF (5′-TCGTCAGCTCGTGTYGTGA-3′) and γ1202R (5′-CGTAAGGGCCATGATG-3′), designed and validated for real-time qPCR by Bacchetti et al. (29). Plasmid pB10::*gfp* was quantified using primers GFP-Fwd (5′-GCCAACACTTGTCACTACTTTC-3′) and GFP-Rev (5′-TGTCTTGTAGTTCCCGTCATC-3′). For each primer pair, the optimal primer concentrations were determined using a 3-by-3 factorial design in which individual primer concentrations were 250, 500, or 750 nM. Except for γ1202R, which had an optimal concentration of 750 nM, all other primers functioned optimally at 250 nM.

For relative quantification of plasmid abundance, the amplification efficiency (E) for both the plasmid- and 16S rRNA gene-specific primer pairs was greater than 1.91, using the slope (m) of a standard curve ($R^2 > 0.99$) constructed from a 10-fold serial dilution of gDNA for each of the three strains (equation 1). The gDNA concentrations in the standard curves ranged from 2×10^1 to 2×10^{-4} ng gDNA per reaction. The abundance (RA) of pB10::*gfp* (P) at a given time point (T_n) relative to T_0 and normalized to the abundance of 16S rRNA genes (16S) at T_n and T_0 was calculated as shown in equations 2 and 3, where Cp is the threshold crossing point and S is the amplicon size. The plasmid/chromosome ratio (P:16S) was calculated by multiplying the output from equation 2 by the number of 16S rRNA gene copies per chromosome. *P. putida* has seven (30) and *P. veronii* three (31) 16S rRNA gene copies per chromosome.

$$E = 10^{\left(-\frac{1}{m}\right)} \tag{1}$$

$$P{:}16\mathrm{S} = \frac{(E_{16S})^{\mathrm{Cp}_{16S}}}{(E_P)^{\mathrm{Cp}_P}} \times \frac{S_{16S}}{S_P} \tag{2}$$

$$\mathrm{RA} = \frac{P{:}16\mathrm{S}_{T_n}}{P{:}16\mathrm{S}_{T_o}} \tag{3}$$

For absolute quantification of the number of chromosomes per reaction, standard curves were constructed using known quantities of pWLE005

(3,302 bp), ranging between ~10^9 and 10^5 molecules per reaction. This vector was constructed by cloning the 16S rRNA gene from *P. putida* UWC-1, using the universal primers 27f (5′-AGAGTTTGATCMTGGCTCAG-3′) and 1492r (5′-TACGGYTACCTTGTTACGACTT-3′), into pJET1.2 using a CloneJET PCR cloning kit (Thermo Scientific) per the manufacturer's instructions. The number of chromosomes in each real-time qPCR was extrapolated from the standard curves using equation 4, where Cp is the threshold crossing point, *y* and *m* are the intercept and slope of the linear regression, respectively, and N_{16S} is the number of 16S rRNA gene copies per chromosome.

$$\text{Number of chromosomes} = \frac{10^{(Cp - y)/m}}{N_{16S}} \quad (4)$$

Statistical analysis. A logistic regression model (32) was used to estimate the rate of decline of plasmid-bearing cells in the population, in part as previously described (33). The model estimates the rate of decrease of the plasmid-bearing fraction in a population over time but does not distinguish between the effects of segregational plasmid loss at cell division, plasmid cost, or horizontal plasmid transfer. Due to the nonlinear nature of this rate, the maximum rate of decline of the plasmid-bearing fraction was used to compare the ability of the different techniques to quantitatively measure differences in plasmid persistence. This maximum rate occurs at the time where the plasmid-bearing fraction of the population is 50% and is loosely defined as the (plasmid) loss rate throughout this study. Markov chain Monte Carlo (MCMC) was used to implement the model, specifically using a Gibbs sampler (34) as implemented in JAGS (35), and convergence was assessed using the Gelman-Rubin diagnostic (36). Computation was done using R, version 2.15.0 (R Development Core Team, 2012; http://www.R-project.org/) utilizing the package rjags (M. Plummer, 2011; http://CRAN.R-project.org/package=rjags) for interface with JAGS and CODA (37) for diagnostics. A more detailed description of logistic regression models can be found in the supplemental material. Statistical comparisons were done utilizing the Welch two-sample *t* test (unpaired), analysis of variance (ANOVA), and variance comparison functions, where appropriate, within the R software package. The stability assay data used in the analysis are included as Data Sets S1 and S2 in the supplemental material.

RESULTS AND DISCUSSION

The natural IncP-1β plasmid pB10 previously was shown to be stable, moderately unstable, and highly unstable in *P. putida* UWC-1, *P. veronii* S34, and *P. putida* H2, respectively (4). Using the same three hosts and a GFP-encoding derivative of pB10, pB10::*gfp*, we set out to determine whether FCM and real-time qPCR can be used as alternative techniques for monitoring plasmid persistence compared to more conventional PC methods. Normally in these conventional assays, the selectable phenotype would be plasmid-encoded antibiotic resistance, and the relative proportions often are determined by replica plating. However, here we used green fluorescence of colonies on nonselective agar plates as an indicator of plasmid presence to avoid the visible bias that otherwise would be introduced in replica plating.

Effect of marker gene insertion in plasmid persistence. To determine possibly confounding effects of plasmid marking on determining plasmid persistence, we compared the persistence of pB10::*gfp* to that of the wild-type (WT) unmarked plasmid pB10 using the PC method. First, just like pB10, pB10::*gfp* persisted extremely well in *P. putida* UWC-1. The difference in plasmids is the insertion of a minitransposon with antibiotic resistance and *gfp* genes into the *kfrB* gene, which may be involved in plasmid inheritance (38). Based on our results, the segregational loss rate of both plasmids must be extremely low in this strain despite the disruption of *kfrB*. Thanks to this apparent low loss rate, additional costly genes on the plasmid did not have a drastic effect on the overall persistence. Second, in *P. veronii* S34 the mean loss rate of pB10::*gfp* was -9.88×10^{-3} per generation compared to only sporadic loss (indistinguishable from 0) of pB10 during the same 10-day period (4) (see Fig. S1 and S2 in the supplemental material) (Welch two-sample *t* test; $t = -63.6086$; df = 29; $P < 0.001$; where *t* is the *t* statistic, df is the degrees of freedom, and the *P* value is the probability that the two data sets are different). It should be noted that in a previous study, the pB10-bearing fraction also rapidly decreased after 10 days, indicating an acceleration of loss for the marked plasmid (4). Lastly, in *P. putida* H2, the mean loss rate for pB10::*gfp* was lower than that for pB10 (-3.11×10^{-2} and 9.85×10^{-2} per generation, respectively; Welch two-sample *t* test; $t = 79.3615$; df = 35.445; $P < 0.001$). However, Fig. S1 in the supplemental material clearly shows that the initial fraction of pB10::*gfp*-containing cells was lower, and that of plasmid-containing cells decreased below detectable levels sooner. Thus, in *P. veronii* S34 and *P. putida* H2, insertion of the GFP-encoding transposon into pB10 seemed to adversely affect plasmid stability. This likely is due to an increase in the plasmid cost through the addition of expressed genes, even though a negative effect of *kfrB* inactivation on plasmid inheritance in these strains, in contrast to UWC-1, cannot be excluded. Insertion of any marker gene that is expressed throughout the assay likely will increase the plasmid's fitness cost, but its effect on segregational loss can be minimized by carefully choosing a suitable locus for insertion.

Plasmid persistence by flow cytometry. We compared the results of plasmid persistence assays as measured by FCM and PC. To monitor the fraction of plasmid-containing cells in each of the three strains by FCM, samples of triplicate populations were interrogated daily for the presence or absence of a GFP phenotype in individual cells. The discriminatory gates were set based on the SSC, FSC, and FITC-A measurements of positive (plasmid-containing) and negative (plasmid-free and blank) control populations (Fig. 1). The absence of a fluorescent phenotype following plasmid loss allowed easy differentiation between plasmid-free (FITC-A^-) and plasmid-containing (FITC-A^+) cells (Fig. 1D to F). The loss of the fluorescent signal after plasmid loss is due to GFP degradation and dilution upon cell division; this may cause a delay between the actual plasmid loss event and complete signal extinction, possibly causing a slight overestimation of the plasmid-containing fraction. Since the plasmid-free and plasmid-bearing cells did not differ much in the SSC and FSC scatter profiles (Fig. 1A to C), these measures were used only to distinguish bacterial cells from the background.

For *P. putida* UWC-1, the persistence profiles (Fig. 2) generated by PC and FCM were very similar, as expected due to the persistent nature of pB10::*gfp* in this strain. As there was no net change in the fraction of plasmid-bearing cells over time when measured using either PC or FCM, the logistic regression model could not be used and the plasmid loss rates were reported as zero (Fig. 3).

In *P. veronii* S34, FCM estimated a slightly lower plasmid loss rate than the moderately low plasmid loss rate observed by PC (-4.01×10^{-3} and -9.75×10^{-3} per generation, respectively; Welch two sample *t* test; $t = -20.2862$; df = 48.466; $P < 0.001$) (Fig. 2 and 3). At the same photomultiplier voltages, the scatter profile of plasmid-containing *P. veronii* S34 cells had a broader distribution across both SSC and FSC, while plasmid-free cells

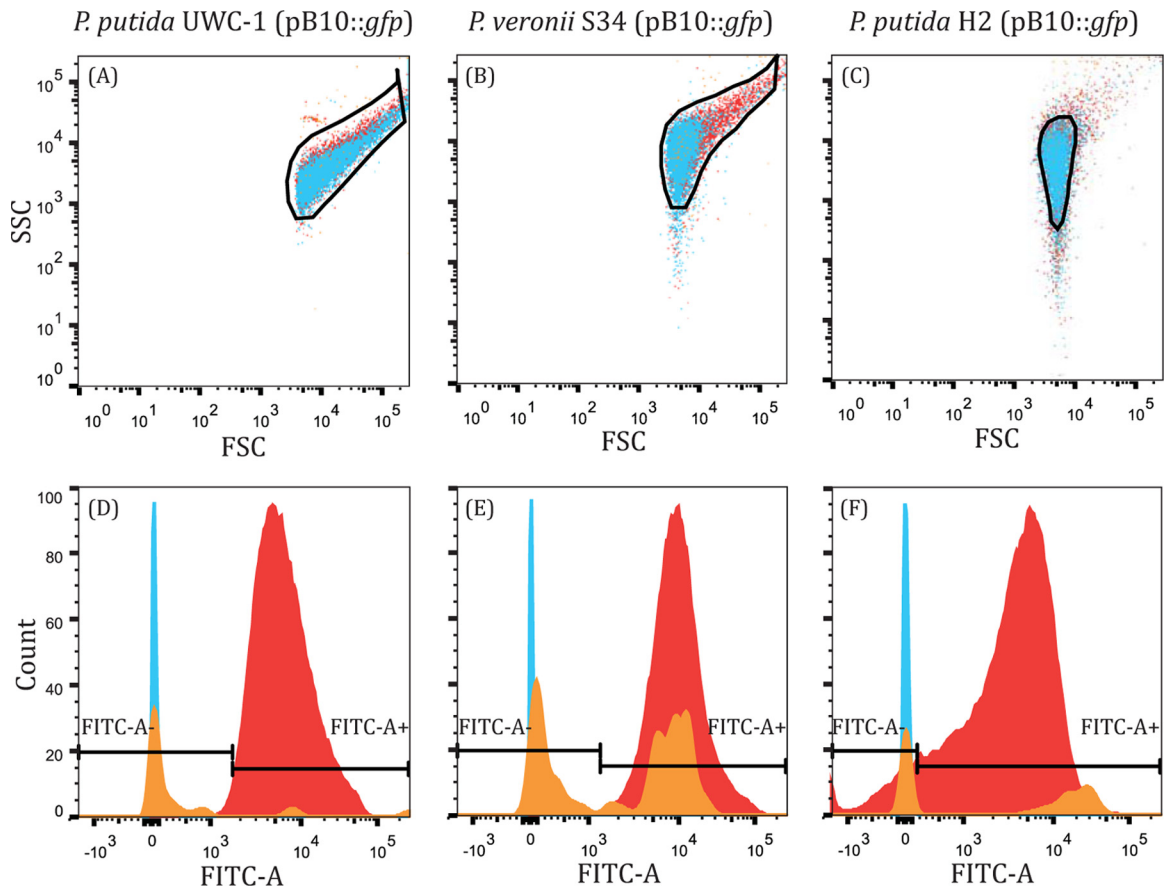

FIG 1 FCM scatter SSC/FSC profiles (A to C) and population count histograms (D to F) clearly showing the plasmid-bearing fluorescent (FITC-A$^+$) (red, right side in panels D to F) and plasmid-free nonfluorescent fractions (FITC-A$^-$) (blue, left side in panels D to F), as well as control populations of *P. putida* UWC-1, *P. veronii* S34, and *P. putida* H2. Initial SSC-FSC gates (black lines) were set using plasmid-containing and plasmid-free control populations as well as a blank sample (orange) to exclude background events. The populations then were further gated on FITC-A such that 99.5% of the plasmid-containing population was FITC-A positive (*P. putida* UWC-1 and *P. veronii* S34) or to best discriminate between the plasmid-containing and -free populations (*P. putida* H2). Thus, the SSC-FSC profiles and histograms for each strain are composites representing individual populations of plasmid-containing (red) and plasmid-free cells (blue) as well as a blank sample (orange).

were distributed more broadly across SSC than FSC (Fig. 1). There was also a noticeable bias toward GFP-positive cells during counting; more plasmid-containing cells were counted than plasmid-free cells in a culture with similar densities of the two respective populations. These factors, combined with the possible delay in loss of fluorescence signal, likely resulted in underestimation of the maximum plasmid loss rate in *P. veronii* S34. Therefore, the ability to accurately measure the frequency of plasmid-containing and -free cells within a population of cells using FCM is contingent upon the ability to discriminate between the two subpopulations without introducing a bias.

The mean rate of plasmid loss in *P. putida* H2, which poorly maintained pB10::*gfp* (Fig. 2), estimated by FCM was only slightly higher than that inferred by PC (3.91×10^{-2} and 3.10×10^{-2} per generation, respectively; Welch two sample t test; $t = 17.0344$; df $= 56.257$; $P < 0.001$) (Fig. 3). In contrast, a larger initial fraction of plasmid-containing cells was recorded by FCM than by PC (Fig. 2). Therefore, we tested the possibility that PC underestimated plasmid presence due to plasmid loss occurring within colonies during growth on the nonselective agar plate. If plasmid loss occurred early during colony growth, fluorescence might not be visible to the naked eye, and such colonies would be mistakenly recorded as plasmid free even though a small fraction still retained the plasmid. To test this, 52 nonfluorescent colonies from each of the 3 replicate *P. putida* H2 (pB10::*gfp*) populations at T_0 were replicated onto plasmid-selective and nonselective media. Of these, 10% ± 2% grew on plates with plasmid-selective antibiotics and displayed the GFP phenotype. Thus, plasmid loss also occurred during colony growth on the nonselective media, resulting in nonfluorescent colonies that were founded by fluorescent plasmid-bearing cells, thereby underestimating their proportion. In conclusion, while the plasmid persistence curves obtained with the two methods did not coincide for two of the strains, they follow the same trend and confirm previous findings that plasmid pB10 can be very stable, moderately unstable, and highly unstable depending on the host (Fig. 2).

Plasmid persistence by real-time qPCR. Real-time qPCR was used to assay plasmid persistence by determining the ratio of plasmid DNA molecules to 16S rRNA gene molecules within total DNA extractions from cells harvested over the course of the persistence assays. The normalized data then were used to determine the abundance of plasmid DNA at a given time point relative to

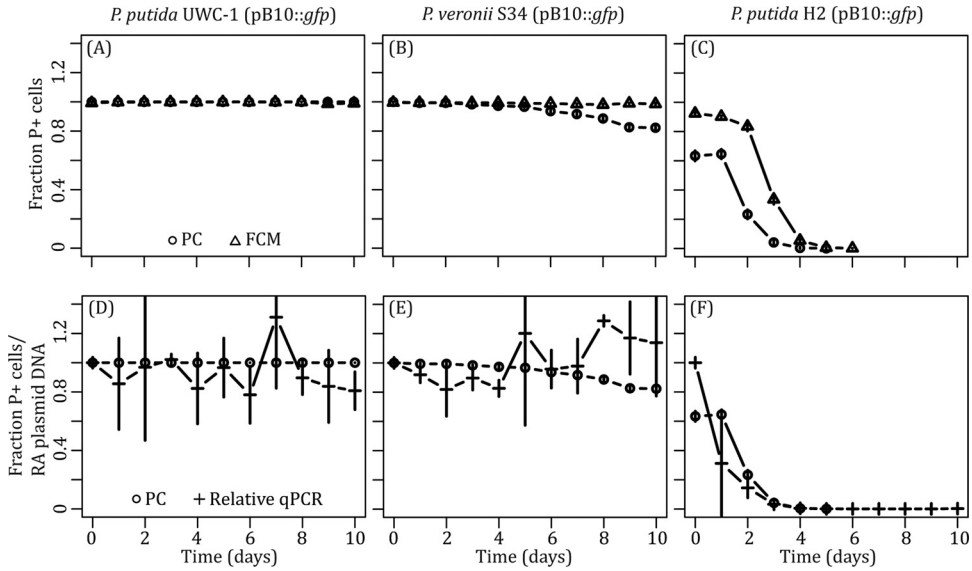

FIG 2 Plasmid persistence measured using FCM (A to C) and real-time qPCR (D to F) compared to PC for each of the three bacterial hosts. Each persistence assay was repeated in triplicate. P+, plasmid-containing; RA, relative abundance.

that at the initial time point as a proxy for plasmid persistence. The persistence profiles of pB10::*gfp* in *P. putida* UWC-1 and *P. veronii* S34 obtained by real-time qPCR were more variable than that by PC. This resulted in a mean loss rate in *P. putida* UWC-1 that was slightly higher (1.163×10^{-3} compared to 0 per generation; Welch two-sample *t* test; $t = 20.0979$; df = 29; $P < 0.001$), while in *P. veronii* S34 it was significantly lower than the estimates based on PC (2.15×10^{-3} and -9.75×10^{-3} per generation, respectively; Welch two-sample *t* test; $t = -66.8335$; df = 52.108; $P < 0.001$) (Fig. 2 and 3). From the PC data it was evident that pB10::*gfp*-free cells were generated rarely, if ever, during the *P. putida* UWC-1 persistence assay. Therefore, it was possible to use the real-time qPCR data from this assay to calculate the average number of plasmids per chromosome for each day without plasmid loss being a factor. The ratio of plasmids to chromosome varied between 1.6 and 3.5 over time (Fig. 4). This was not significantly different from the variation in the plasmid/chromosome ratio within genomic DNA extracted in triplicate from the same frozen *P. putida* UWC-1(pB10::*gfp*) population on two different days (pairwise *t* test; df = 12; $F = 1.079$; $P = 0.416$). Thus, the fluctuation in plasmid abundance observed in *P. putida* UWC-1 and *P. veronii* S34 was likely the result of experimental error during genomic DNA extraction. Increasing the number of replicates to five per sample at the expense of sampling frequency did not make a meaningful difference (results not shown). However, due to changes in the physiological state of the culture over time, it is also possible that fluctuations in plasmid copy number have a similar effect when using real-time qPCR to measure plasmid persistence. In spite of the variation, when combined with a logistic regression model as done here, it is still possible to infer the overall ability of a plasmid to persist.

In a host such as *P. putida* H2, where plasmid persistence was

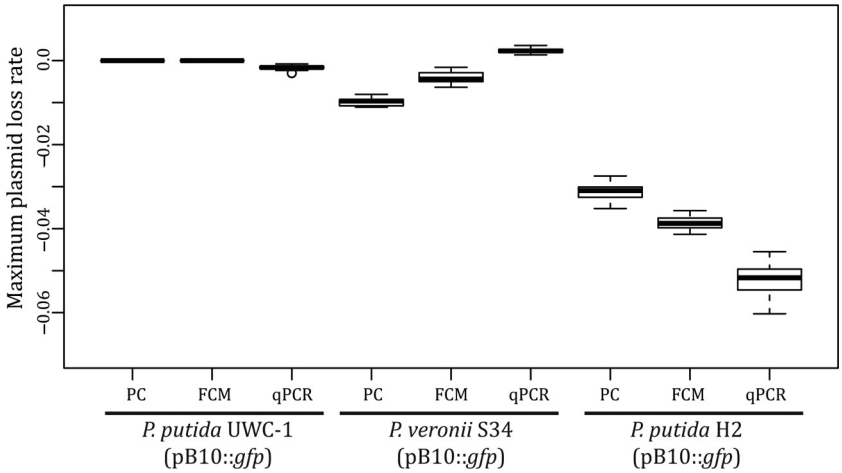

FIG 3 Maximum plasmid loss rates calculated based on the data obtained by the three techniques. This rate represents the average rate of change in the fraction of plasmid-containing cells (PC and FCM) or in the normalized abundance of plasmid DNA (real-time qPCR) per generation at the time point where 50% of the population was plasmid free.

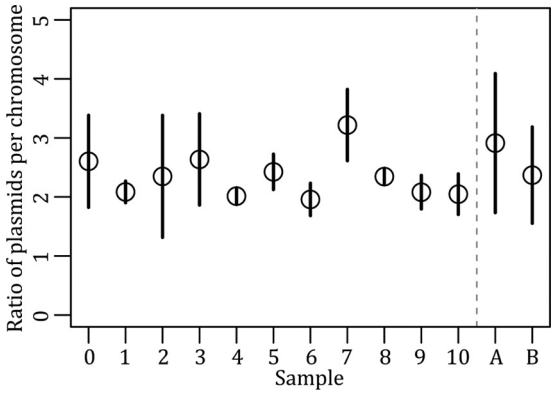

FIG 4 Fluctuations in the number of pB10::*gfp* plasmids per chromosome averaged across three replicate *P. putida* UWC-1 populations for each day of the persistence assay (samples 1 to 10) compared to the average ratio of plasmids per chromosome in triplicate genomic DNAs extracted on two different days from the same archived culture of UWC-1 (pB10::*gfp*) (samples A and B).

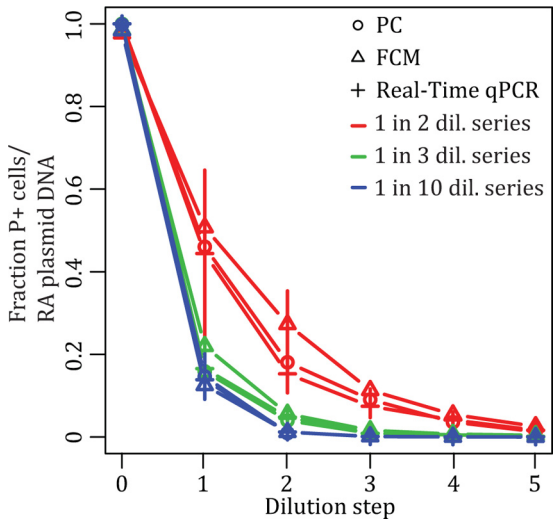

FIG 5 Artificial plasmid persistence assays, consisting of mixtures of plasmid-containing and -free *P. putida* UWC-1 cells at known ratios and measured by PC, FCM, and real-time qPCR. Different artificial plasmid loss rates were obtained by serially diluting cultures of plasmid-containing cells into cultures of plasmid-free cells 5 times following a 1:2, 1:3, and 1:10 dilution (dil.) series, performed in triplicate. P+, plasmid containing; RA, relative abundance. See Fig. S4 in the supplemental material for the same results displayed on a logarithmic scale.

poor, there was less fluctuation in the ratio of plasmid to chromosome over time. The result of the real-time qPCR measurements was a curve that indicated rapid plasmid loss (Fig. 2), and the mean loss rate was only slightly higher than that by PC (5.15×10^{-2} and 3.11×10^{-2} per generation, respectively; Welch two sample t test; $t = 28.0541$; df $= 43.567$; $P < 0.001$) (Fig. 3). A significant advantage of this technique was that pB10::*gfp* could be detected within the *P. putida* H2 population for the entire 10-day period. When measured by PC and FCM, the fraction of plasmid-containing cells decreased below detectable levels within 5 to 6 days, respectively. Each 2-ng *P. putida* H2 genomic DNA sample contained $4.62 \times 10^7 \pm 1.54 \times 10^7$ chromosomes (see Fig. S3 in the supplemental material). Assuming one chromosome per cell, the sample size screened by real-time qPCR was $\sim 1.86 \times 10^5$- and $\sim 8.71 \times 10^2$-fold greater than that screened by PC and FCM, respectively; this explains the ability to detect the plasmid even at very low abundances (Fig. 2). It should be noted, however, that stationary-phase cells often contain more than one chromosome per cell (39); thus, the sample size likely is overestimated 2- to 8-fold. Nonetheless, real-time qPCR provides a much larger dynamic range for measuring plasmid persistence than PC and FCM. Although such a high dynamic range is not required to capture plasmid loss rates in most experiments, it allows measuring the persistence of a plasmid even when it occurs in only a small fraction of a bacterial population or community.

Resolution. The ability to resolve small differences in plasmid persistence becomes especially important when investigating the effect of specific genes, mutations, or hosts on the plasmid loss rate. To compare the resolving ability of FCM and real-time qPCR to that of the PC method, we constructed and analyzed three artificial persistence assays using *P. putida* UWC-1 cells with and without pB10::*gfp* (Fig. 5). In these assays, the plasmid-containing bacterial culture was diluted into a plasmid-free culture following either a 1:2, 1:3, or 1:10 dilution series to obtain slopes which, in theory, are equivalent to plasmid loss rates (change in fraction of plasmid-bearing cells per dilution) of −0.075, −0.119, and −0.250, respectively, and representing relative rate differences of 1.59-fold (1:3 versus 1:2), 2.10-fold (1:10 versus 1:3), and 3.32-fold (1:10 versus 1:2). The three techniques yielded mean loss rates that were similar but not identical to each other (Fig. 6; also see Table S1 in the supplemental material), yet they all were able to statistically resolve the relatively small differences in loss rates (see Table S2). The variation in the estimated maximum loss rates introduced by each technique generally was similar between the three methods (see Table S3). Thus, all three methods were capable of resolving the small differences in these artificial persistence assays.

Conclusions. Both FCM and real-time qPCR were successfully applied to monitor the persistence of pB10::*gfp* in three different bacterial hosts compared to a more conventional PC assay. Although more sample processing was required (thereby also increasing the cost per sample), real-time qPCR, unlike PC and FCM, does not require any selectable markers to be present on the plasmid and provides the highest dynamic range. Thus, real-time qPCR-based measurement of plasmid persistence would allow monitoring the persistence of resistance as well as so-called cryptic plasmids even at low abundance, as long as partial DNA sequence is available. The caveat to this technique was the fluctuation in the data in cases where there was little to no plasmid loss. Current statistical models for separating the effects of segregational loss, cost, and transfer on plasmid persistence have been developed previously within our group, but currently they rely on measurements of the actual frequencies of plasmid-containing and -free cells within a population (19, 40). Adaptation of these models to use the relative abundance of plasmid DNA as measured in this study will further increase the usefulness of real-time qPCR for the purposes of quantitatively measuring and defining plasmid persistence.

In contrast to real-time qPCR, FCM interrogates individual cells within a population for the presence or absence of a plasmid-encoded phenotype, making the data more suitable for our existing models. However, FCM is not without its caveats. Differences in the SSC and FSC scatter profiles of plasmid-containing and

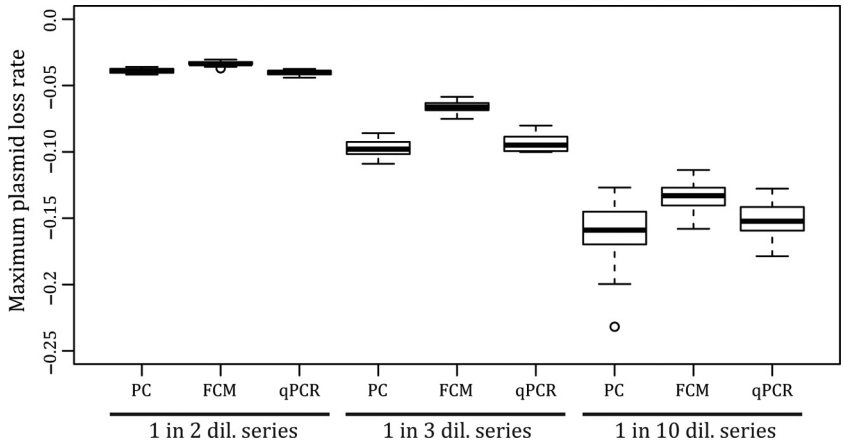

FIG 6 Maximum plasmid loss rate measured by PC, FCM, and real-time qPCR for the three artificial plasmid persistence assays consisting of known ratios of plasmid-containing and -free cells. Rates are expressed as per-generation values to make them comparable to the rates estimated from real persistence assays, with a dilution cycle being equivalent to 1 day, i.e., 10 generations, in the serial batch cultures.

-free cells or differences in fluorescence intensity due to GFP instability or autofluorescence within cells can result in biased counting and, therefore, under- or overestimations of plasmid stability. There is also an unavoidable metabolic cost associated with expression of the heterologous GFP and a potential gene loss or mutations during long-term cultivation. An alternative FCM-based strategy that negates the need for plasmid-encoded markers is the use of fluorescently labeled antibodies to recognize plasmid-specific antigens. This would, however, limit such assays to plasmids that express surface-located proteins and would drastically increase the sample preparation time.

The differences in loss rates measured by FCM and real-time qPCR within plasmid persistence assays with *P. veronii* S34 and *P. putida* H2 (Fig. 3) were not observed in the artificial persistence assays (Fig. 6). This suggests that these loss rate differences were not related to the methods themselves but rather were due to changes in the bacterial cells over time that affected the FCM and real-time qPCR-based measurements in different ways.

Finally, although FCM appeared to introduce slightly less variance in the estimated maximum loss rates compared to real-time qPCR, both techniques were found to be suitable for resolving small differences in plasmid stability. Thus, given the growing need for high-throughput methods, both FCM and real-time qPCR technologies are candidate methods for the routine measurement of plasmid persistence in high-throughput formats with the additional advantage of high resolution and dynamic range. Given the drawback of inserting a fluorescent marker gene for FCM, we recommend qPCR as the best high-throughput method for monitoring plasmid persistence.

ACKNOWLEDGMENTS

This work was funded by the National Institute of Allergy and Infectious Diseases (NIAID) of the National Institutes of Health (NIH grant R01 AI084918) and the United States Department of Defense (award number DM110149). Additional support was provided by the IBEST Core Facilities, funded by a Center of Biomedical Research Excellence grant (GM10332401) from the National Institute of General Medical Sciences of the National Institutes of Health.

We thank Zaid Abdo for previously developing the logistic regression model and Ranae Shrum for helpful discussions on statistical methods.

REFERENCES

1. **Thomas CM.** 2000. Paradigms of plasmid organization. Mol. Microbiol. **37:**485–491. http://dx.doi.org/10.1046/j.1365-2958.2000.02006.x.
2. **Bingle LE, Thomas CM.** 2001. Regulatory circuits for plasmid survival. Curr. Opin. Microbiol. **4:**194–200. http://dx.doi.org/10.1016/S1369-5274(00)00188-0.
3. **Bouma JE, Lenski RE.** 1988. Evolution of a bacteria/plasmid association. Nature **335:**351–352. http://dx.doi.org/10.1038/335351a0.
4. **De Gelder L, Ponciano JM, Joyce P, Top EM.** 2007. Stability of a promiscuous plasmid in different hosts: no guarantee for a long-term relationship. Microbiology **153:**452–463. http://dx.doi.org/10.1099/mic.0.2006/001784-0.
5. **De Gelder L, Williams JJ, Ponciano JM, Sota M, Top EM.** 2008. Adaptive plasmid evolution results in host-range expansion of a broad-host-range plasmid. Genetics **178:**2179–2190. http://dx.doi.org/10.1534/genetics.107.084475.
6. **Friehs K, Reardon KF.** 1993. Parameters influencing the productivity of recombinant *E. coli* cultivations. Adv. Biochem. Eng. Biotechnol. **48:**53–77.
7. **Sota M, Yano HHM, Daughdrill JGW, Abdo Z, Forney LJ, Top EM.** 2010. Shifts in the host range of a promiscuous plasmid through parallel evolution of its replication initiation protein. ISME J. **4:**1568–1580. http://dx.doi.org/10.1038/ismej.2010.72.
8. **Gillings MR.** 2013. Evolutionary consequences of antibiotic use for the resistome, mobilome and microbial pangenome. Front. Microbiol. 4: http://dx.doi.org/10.3389/fmicb.2013.00004.
9. **Kåhrström CT.** 2013. Entering a post-antibiotic era? Nat. Rev. Microbiol. 11:146. http://dx.doi.org/10.1038/nrmicro2983.
10. **San Millan A, Heilbron K, Maclean RC.** 2014. Positive epistasis between co-infecting plasmids promotes plasmid survival in bacterial populations. ISME J. **8:**601–612. http://dx.doi.org/10.1038/ismej.2013.182.
11. **Bonot S, Merlin C.** 2010. Monitoring the dissemination of the broad-host-range plasmid pB10 in sediment microcosms by quantitative PCR. Appl. Environ. Microbiol. **76:**378–382. http://dx.doi.org/10.1128/AEM.01125-09.
12. **Cooper TF, Heinemann JA.** 2000. Postsegregational killing does not increase plasmid stability but acts to mediate the exclusion of competing plasmids. Proc. Natl. Acad. Sci. U. S. A. **97:**12643–12648. http://dx.doi.org/10.1073/pnas.220077897.
13. **Deane SM, Rawlings DE.** 2004. Plasmid evolution and interaction between the plasmid addiction stability systems of two related broad-host-range IncQ-like plasmids. J. Bacteriol. **186:**2123–2133. http://dx.doi.org/10.1128/JB.186.7.2123-2133.2004.
14. **Guynet C, Cuevas A, Moncalián G, de la Cruz F.** 2011. The *stb* operon balances the requirements for vegetative stability and conjugative transfer of plasmid R388. PLoS Genet. **7:**e1002073. http://dx.doi.org/10.1128/AEM.01125-09.

15. **Heuer H, Fox RE, Top EM.** 2007. Frequent conjugative transfer accelerates adaptation of a broad-host-range plasmid to an unfavorable *Pseudomonas putida* host. FEMS Microbiol. Ecol. **59:**738–748. http://dx.doi.org/10.1111/j.1574-6941.2006.00223.x.
16. **Popov M, Petrov S, Nacheva G, Ivanov I, Reichl U.** 2011. Effects of a recombinant gene expression on ColE1-like plasmid segregation in *Escherichia coli*. BMC Biotechnol. **11:**18. http://dx.doi.org/10.1186/1472-6750-11-18.
17. **Wegrzyn K, Witosinska M, Schweiger P, Bury K, Jenal U, Konieczny I.** 2013. RK2 plasmid dynamics in *Caulobacter crescentus* cells–two modes of DNA replication initiation. Microbiology **159:**1010–1022. http://dx.doi.org/10.1099/mic.0.065490-0.
18. **Tal S, Paulsson J.** 2012. Evaluating quantitative methods for measuring plasmid copy numbers in single cells. Plasmid **67:**167–173. http://dx.doi.org/10.1016/j.plasmid.2012.01.004.
19. **Lau BT, Malkus P, Paulsson J.** 2013. New quantitative methods for measuring plasmid loss rates reveal unexpected stability. Plasmid **70:**353–361. http://dx.doi.org/10.1016/j.plasmid.2013.07.007.
20. **Bahl MI, Hansen LH, Licht TR, Sørensen SJ.** 2007. Conjugative transfer facilitates stable maintenance of IncP-1 plasmid pKJK5 in *Escherichia coli* cells colonizing the gastrointestinal tract of the germfree rat. Appl. Environ. Microbiol. **73:**341–343. http://dx.doi.org/10.1128/AEM.01971-06.
21. **Bahl MI, Sørensen SJ, Hestbjerg Hansen L.** 2004. Quantification of plasmid loss in *Escherichia coli* cells by use of flow cytometry. FEMS Microbiol. Lett. **232:**45–49. http://dx.doi.org/10.1016/S0378-1097(04)00015-1.
22. **Rysz M, Mansfield WR, Fortner JD, Alvarez PJ.** 2013. Tetracycline resistance gene maintenance under varying bacterial growth rate, substrate and oxygen availability, and tetracycline concentration. Environ. Sci. Technol. **47:**6995–7001. http://dx.doi.org/10.1021/es3035329.
23. **Shintani M, Matsui K, Inoue J, Hosoyama A, Ohji S, Yamazoe A, Nojiri H, Kimbara K, Ohkuma M.** 2014. Single-cell analyses revealed transfer ranges of IncP-1, IncP-7, and IncP-9 plasmids in a soil bacterial community. Appl. Environ. Microbiol. **80:**138–145. http://dx.doi.org/10.1128/AEM.02571-13.
24. **Van Meervenne E, Van Coillie E, Kerckhof FM, Devlieghere F, Herman L, De Gelder LS, Top EM, Boon N.** 2012. Strain-specific transfer of antibiotic resistance from an environmental plasmid to foodborne pathogens. J. Biomed. Biotechnol. **2012:**834598. http://dx.doi.org/10.1155/2012/834598.
25. **McClure NC, Weightman AJ, Fry JC.** 1989. Survival of *Pseudomonas putida* UWC1 containing cloned catabolic genes in a model activated-sludge unit. Appl. Environ. Microbiol. **55:**2627–2634.
26. **De Gelder L, Vandecasteele FPJ, Brown CJ, Forney LJ, Top EM.** 2005. Plasmid donor affects host range of promiscuous IncP-1beta plasmid pB10 in an activated-sludge microbial community. Appl. Environ. Microbiol. **71:**5309–5317. http://dx.doi.org/10.1128/AEM.71.9.5309-5317.2005.
27. **Ausubel FM, Brent R, Kingston RE, Moore DD, Seidman JG, Smith JA, Struhl K.** 1993. Current protocols in molecular biology. Wiley Interscience, New York, NY.
28. **Sambrook J, Fritsch EF, Maniatis T.** 1989. Molecular cloning, a laboratory manual. Cold Spring Harbor Laboratory Press, Cold Spring Harbor, NY.
29. **Bacchetti De Gregori T, Aldred N, Clare AS, Burgess JG.** 2011. Improvement of phylum- and class-specific primers for real-time PCR quantification of bacterial taxa. J. Microbiol. Methods **86:**351–356. http://dx.doi.org/10.1016/j.mimet.2011.06.010.
30. **Bodilis J, Nsigue-Meilo S, Besaury L, Quillet L.** 2012. Variable copy number, intra-genomic heterogeneities and lateral transfers of the 16S rRNA gene in *Pseudomonas*. PLoS One **7:**e35647. http://dx.doi.org/10.1371/journal.pone.0035647.
31. **De Lima-Morales D, Chaves-Moreno D, Jarek M, Vilchez-Vargas R, Jauregui R, Pieper DH.** 2013. Draft genome sequence of *Pseudomonas veronii* strain 1YdBTEX2. Genome Announc. **1:**e00258-13. http://dx.doi.org/10.1128/genomeA.00258-13.
32. **Gelman A.** 2007. Data analysis using regression and multilevel/hierarchical models. Cambridge University Press, Cambridge, United Kingdom.
33. **Hughes JM, Lohman BK, Deckert GE, Nichols EP, Settles M, Abdo Z, Top EM.** 2012. The role of clonal interference in the evolutionary dynamics of plasmid-host adaptation. mBio **3:**e00077–12. http://dx.doi.org/10.1128/mBio.00077-12.
34. **Geman S, Geman D.** 1984. Stochastic relaxation, Gibbs distributions, and the Bayesian restoration of images. IEEE Trans. Pattern Anal. Mach. Intell. **6:**721–741.
35. **Plummer M.** 2003. JAGS: a program for analysis of Bayesian graphical models using Gibbs sampling. *In* Hornik K, Leisch F, Zeileis A (ed), Proceedings of the 3rd International Workshop on Distributed Statistical Computing, Vienna, Austria.
36. **Geweke J.** 1992. Evaluating the accuracy of sampling-based approaches to calculating posterior moments. *In* Bernardo JM, Berger JO Dawid AP Smith AFM (ed), Bayesian statistics 4. Oxford, University Press, Oxford, United Kingdom.
37. **Plummer M, Best N, Cowles K, Vines K.** 2006. CODA: convergence diagnosis and output analysis for MCMC. R News **6:**7–11.
38. **Adamczyk M, Dolowy P, Jonczyk M, Thomas CM, Jagura-Burdzy G.** 2006. The *kfrA* gene is the first in a tricistronic operon required for survival of IncP-1 plasmid R751. Microbiology **152:**1621–1637. http://dx.doi.org/10.1099/mic.0.28495-0.
39. **Åkerlund T, Nordström K, Bernander R.** 1995. Analysis of cell size and DNA content in exponentially growing and stationary-phase batch cultures of *Escherichia coli*. J. Bacteriol. **177:**6791–6797.
40. **Ponciano JM, De Gelder L, Top EM, Joyce P.** 2007. The population biology of bacterial plasmids: a hidden Markov model approach. Genetics **176:**957–968. http://dx.doi.org/10.1534/genetics.106.061937.